

R. Pampin, A. Davis

Novel tools for estimation of activation dose: description, preliminary comparison and nuclear data requirements

Enquiries about copyright and reproduction should in the first instance be addressed to the Culham Publications Officer, Culham Centre for Fusion Energy (CCFE), Library, Culham Science Centre, Abingdon, Oxfordshire, OX14 3DB, UK. The United Kingdom Atomic Energy Authority is the copyright holder.

Novel tools for estimation of activation dose: description, preliminary comparison and nuclear data requirements

R. Pampin, A. Davis

EURATOM/UKAEA Fusion Association, Culham Science Centre, OX14 3DB, Abingdon, UK

UKAEA FUS 549

EURATOM/UKAEA Fusion

**Novel Tools for Estimation of Activation
Dose: Description, Preliminary
Comparison and Nuclear Data
Requirements**

R. Pampin, A. Davis

July 2008

© UKAEA

EURATOM/UKAEA Fusion Association
Culham Science Centre
Abingdon
Oxfordshire
OX14 3DB
United Kingdom

Telephone: +44 1235 466586
Fax: +44 1235 466435

UKAEA



NEUTRONICS AND NUCLEAR DATA GROUP
TECHNICAL REPORT

JULY 2008

**NOVEL TOOLS FOR ESTIMATION OF ACTIVATION DOSE:
DESCRIPTION, PRELIMINARY COMPARISON AND
NUCLEAR DATA REQUIREMENTS**

R. PAMPIN¹, A. DAVIS^{1,2}

(1) Euratom/UKAEA Fusion Association, Culham Science Centre, Abingdon OX14 3DB, UK

*(2) University of Birmingham, School of Physics and Astronomy, Edgbaston, Birmingham
B15 2TT, UK*



Version 1		
Main author	R. Pampin	14.07.08
Checked by	R. Forrest	16.07.08
Cleared by	I. Cook	22.07.08

CONTENTS

I.	INTRODUCTION	3
II.	MC-R2S ACTIVATION SOURCE GENERATOR	4
III.	ATTILA ACTIVATION SOURCE GENERATOR	6
	FORNAX default nuclear data	6
IV.	1D TEST PROBLEM	9
V.	RESULTS AND ANALYSIS	10
VI.	IMPROVING ATTILA NUCLEAR DATA	12
VII.	DISCUSSION	14
	REFERENCES	15
	FIGURES	17
	APPENDIX 1: MC-R2S FUNCTIONALITY	27
	APPENDIX 2: ATTILA ASG DESCRIPTION	29
	APPENDIX 3: THE CONTACT DOSE APPROXIMATION IN FISPACT	35

NOVEL TOOLS FOR THE ESTIMATION OF ACTIVATION DOSE: DESCRIPTION, PRELIMINARY COMPARISON AND NUCLEAR DATA REQUIREMENTS

R. Pampin¹, A. Davis^{1,2}

(1) *Euratom/UKAEA Fusion Association, Neutronics and Nuclear Data Group, Abingdon UK.*

(2) *University of Birmingham, School of Physics and Astronomy, Birmingham UK.*

Two different tools for the estimation of activation dose in ITER and fusion devices based on the rigorous-two-step formalism are presented and compared in a simple geometry and irradiation conditions. The tools, one in-house and one commercially available, are based on the two main numerical methods used in radiation transport, Monte Carlo and discrete ordinates respectively. They couple transport and activation calculations in an integrated manner, allowing for the necessarily fine energy and spatial resolution required for this kind of analyses. The accuracy and completeness of the nuclear data of the commercial software is assessed against the well-established EAF data. The test problem is essentially 1D, and ITER-like irradiation conditions are employed. Despite differences in input nuclear data and output isotopic and photon production, activation dose results at several decay times and two different locations are within 15% of each other; this shows the robustness of the methods and the adequacy of the default activation data in ATTILA for shutdown dose calculations under these undemanding conditions. Recommendations are given for the improvement of the nuclear data for other applications.

I. INTRODUCTION

The experimental nature and radiation source intensity of the ITER tokamak pose stringent requirements on occupational safety assessment during the design and commissioning process, represented by the ALARA principle, which are severely complicated by the intricate geometry and large, distributed neutron source. The estimation and minimisation of radiation dose fields in all areas of the machine is a key part of the engineering effort in ITER systems, and fast and reliable tools to perform this task are essential.

On-load neutron and neutron-induced prompt photon dose fields arise from DT reactions during plasma operation; the plasma is a localised source and these doses are relatively straightforward to calculate using standard neutron transport tools such as MCNP [1] or ATTILA [2]. The so-called “off-load”, “decay” or “activation” dose arises from the decay and gamma emission of radionuclides generated during operation via neutron activation of materials around the plasma source. Unlike the on-load fields, decay dose is present even when the machine is shut down; for this reason it is sometimes also referred to as “shutdown” dose. It is absent before irradiation and builds up gradually during operation as a result of the generation of radionuclides.

Except for very lengthy and intense irradiations, shutdown dose is generally lower in magnitude than its on-load neutron and photon counterparts. Neutrons, however, are uncharged and travel deep into the structures and tokamak systems; the activation source is

therefore distributed over the entire machine and is much more difficult to model, making this type of calculation hard to approach. For this reason, estimation of the decay gamma dose has been traditionally made using the semi-infinite slab approximation implemented in activation inventory codes such as FISPACT, [3]. This approximation, however, is known to severely over or under-estimate the activation dose field under very common circumstances. Over the last few years, a more accurate method has been devised and is now commonly accepted by the activation community; this is the so-called “rigorous-two-step” method or R2S, [4], which involves:

- a neutron transport calculation to ascertain the neutron field distribution throughout the geometry of interest due to the plasma source;
- an activation calculation using the neutron field data and irradiation history details to estimate the amount of radionuclides generated in the materials and generate a decay photon source distributed throughout the geometry;
- a photon transport run to ascertain the photon field arising from such source and estimate the dose field due to these decay photons.

Due to the complexity of the geometry and of the neutron and activation field distribution throughout the machine, the spatial resolution of these analyses needs to be fine enough to account for hot spots appearing due to penetrations and thin streaming paths. Moreover, high energy resolution is also required for the proper estimation of activation properties in fusion conditions, which must account for subtle intricacies in the energy dependence of neutron interaction cross-sections such as the so-called “resonances”. Until recently, no tool existed having the integrated capability to rapidly and reliably perform R2S calculations with the spatial and energy resolutions required in ITER. Ideally, such tool should be able to compute the neutron, activation and decay photon fields with the required resolution, and build a highly distributed source covering the entire geometry of interest for use in a photon run that determines the shutdown dose field within the same geometry. If possible, the tool should also allow for the use of this activation source in a problem having different boundary conditions to the geometry of interest; this would make it useful not only for in-situ analyses but also for the assessment of the dose field during transport and storage of activated components. This kind of tool has become known as an activation source generator, or ASG.

Two such ASG tools have become available recently: the in-house MC-R2S system, based on the common MCNP code and the also in-house FISPACT software, [3], and a tool based on the commercial ATTILA code. These tools are therefore based on the two most widely employed numerical methods used to tackle radiation transport problems: Monte Carlo and discrete ordinates. ATTILA has recently started a quality assurance (QA) benchmark exercise process following NEA recommendations, [5]; MC-R2S is still at a preliminary (“alpha”) stage but such benchmark test is also anticipated as necessary. As a first step, however, a simple comparison exercise has been devised in order to start gaining experience on the use of these tools and assess their robustness and limitations. Of particular interest is the assessment of the validity of ATTILA activation data, for which comparison with FISPACT and the EAF libraries is necessary.

II. MC-R2S ACTIVATION SOURCE GENERATOR

UKAEA Fusion acknowledges the importance of developing fast and reliable software to assist the needs of its ITER-related neutronics activities such as shutdown dose calculations. Since recently, it has devoted resources to start the development of an in-house ASG tool. The MC-R2S software (Mesh-tally Coupled Rigorous 2 Step) is a preliminary version of such a tool using the conventional MCNP code and the in-house FISPACT activation code and EAF nuclear data libraries to perform shutdown dose analyses following the R2S formalism.

The necessary energy resolution is guaranteed by the continuous energy treatment of MCNP in the neutron runs and the possibility to perform calculations in fine energy formats with EAF data in FISPACT, [6]; libraries with up to 315 groups are available, although 175 is the standard. The latest edition of the EAF libraries contains information for 2231 nuclides; reactions accounted for are (n,g), (n,2n), (n,3n), (n,a), (n,p), (n,h), (n,d), (n,t), (n,n'p), (n,n'd), (n,n'a), (n,2p), (n,n'), (n,f) and many others, up to 86 different reaction types – see Table 1 for details. The required spatial resolution is accomplished through the use of MCNP mesh tallies as the basis of the neutron, activation and photon analyses and results. Therefore, MC-R2S relies on the powerful Monte Carlo method and the well-established MCNP code to perform the transport analyses, and on the thoroughly tested FISPACT and evaluated EAF data for the activation step; details of these can be found in the user manuals, [1,3].

MC-R2S is a suite of UNIX script and FORTRAN routines coupling MCNP and FISPACT to perform the two transport and one activation calculations in the R2S method (see Figure 1). The MC-R2S suite processes the output of a standard MCNP neutron mesh tally to obtain neutron spectra at every voxel location, the only conditions on the mesh tally being that it must have rectangular geometry and be binned in energy to the VITAMIN-J standard. An additional MCNP run must be performed with the PTRAC output turned on, and from the PTRAC output file the distribution of different materials throughout the mesh is determined. Together with user-specified data such as the irradiation schedule, decay times and material compositions contained within the mesh volume, the script creates an appropriately mixed composition for each voxel location, which is passed to the inventory code FISPACT. Thus the activation section of the code automates the creation of FISPACT input files with appropriately weighted materials, decay times, and irradiation histories for each voxel. FISPACT is called to perform the activation runs. The FISPACT output of interest is the gamma-ray spectra at each decay time step; these spectra are also automatically extracted from the output files and combined to define a spatially and energetically dependent decay gamma source for the subsequent, final MCNP photon run. The source definition is output in standard MCNP SDEF card format, and so there is no need for re-compilation of MCNP. Appendix 1 outlines the functionality of MC-R2S.

Table 1: summary of cross section information in EAF and ATTILA activation data.

no. of reactions	EAF 2007	FORNAX XML	FENDL 2.1	FORNAX + FENDL
n,g	1054	850	63	913
n,a	1045	78	63	141
n,p	1063	52	63	115
n,h	1020	0	0	0
n,d	1077	0	63	63
n,t	1102	0	63	63
n,2n	1059	25	63	88
n,3n	1079	18	63	81
n,f	102	35	63	98
others	56,964	0	0	0
total	65,565	980	504	1484
no. types	86	6	8	8
no. groups	175	3	175	3 or 175
no. nuclide	2231	1312	63	1312
energy	0 – 60 MeV	0 – 20 MeV	0 – 20 MeV	0 – 20 MeV

III. ATTILA ACTIVATION SOURCE GENERATOR

ATTILA is a multi-group energy, neutron-gamma discrete ordinates transport code available from Transpire Inc., using P_N scattering, S_N angular treatment and 3D, unstructured, tetrahedral grids in RTT format. It allows for a wide variety of controls over the mesh, neutron source, cross section libraries, boundary conditions, energy treatment, transport modelling, solver methodology and output production. It is equipped with an automatic mesh generator which accepts CAD input in parasolid (.x_t) and ACIS (.sat) formats. Mesh size can vary by orders of magnitude throughout the computational domain. Tetrahedral elements can be highly anisotropic, enabling adequate directional resolution as well. The code incorporates a multi-group (175 neutron + 42 photon) version of the FENDL 2.1 fusion-specific nuclear data library in DTF format, and is equipped with a 3D graphics tool (TECPLOT) again using CAD format to plot and post-process results. Its neutron and photon transport capabilities have been thoroughly and successfully benchmarked with other radiation transport tools in fusion applications over the last few years, including MCNP and TORT [7,8,9].

ATTILA now has a built-in activation capability based on the R2S formalism and FORNAX transmutation module, which tracks the population of isotopes created through nuclear activation and decay processes. A gamma-ray source specification is produced that represents radiation emitted by decaying nuclides; so it is essentially an ASG. It can be run in a pseudo-time dependent mode where the irradiating flux can be scaled at each time interval. A unique activation source is computed in each tetrahedral element; the complete, distributed activation source throughout the geometry can thus be calculated with the spatial resolution of the finite element mesh and the energy resolution available in the nuclear library. The code uses the FENDL reaction rate data when available, and a user-specific XML file for decay chains and nuclides outside the FENDL library. The functionality of ATTILA's ASG and formulation of the FORNAX solver are described in Appendix 2.

FORNAX default nuclear data

As discussed in Appendix 2, FORNAX is essentially a transmutation matrix solver; construction of the matrix requires detailed information on various nuclear properties. During an activation calculation with FORNAX the transport cross sections are used when available. Currently, the ATTILA FENDL 2.1 data includes 63 stable nuclides (plus 20 elements) and (n,g), (n,2n), (n,3n), (n,a), (n,d), (n,p), (n,t) and (n,f) reaction cross sections in 175 groups. However, activation inventory estimation normally requires data for a much wider range of nuclides. Since this information may not be readily available to users, FORNAX includes a default transmutation database in XML format based on the ORIGEN-S light-element, actinide, and fission product libraries, [10,11]. The default data set contains three group reaction cross sections (thermal, resonance and fast), decay constants, branching fractions, gamma lines and fission yields, as well as other transmutation information for 1312 isotopes, including some 170 metastable. An example of FORNAX XML nuclide listing is shown in Figure 2. Reactions included in the XML file are (n,g), (n,2n), (n,3n), (n,a), (n,p), and (n,f) – see Table 1 again for details. Table 2 lists the 1312 isotopes in the default XML file: 1305 from the ORIGEN-S library plus 7 added by Transpire. This default database contains a significant amount of data some of which is of undetermined pedigree, and thus no warranty can be made as to the accuracy and completeness of this data. It is possible, however, to replace or modify the FORNAX XML default library data with user-specified data.

Of the above 1312 nuclides, 1032 are common to the EAF libraries. Figure 3 is a plot of the ratio of the EAF to FORNAX half-life values for the 1032 common nuclides. The remaining 280 nuclides in the XML file are not found in EAF data; these are mostly actinides and fission products of little relevance to fusion applications. There are also 1198 nuclides in the EAF libraries not present in FORNAX XML.

Table 2: the 1312 nuclides included in the FORNAX XML default nuclear data.

	AR 37	NI 62	GE 73	BR86M	SR 100	NB 108	RU 114	AG 111M	IN 122
	AR 38	NI 63	GE73M	BR 87	SR 101	NB 109	RU 115	AG 112	IN 122M
	AR 39	NI 64	GE 74	BR 88	SR 102	NB 110	RU 116	AG 113	IN 123
H 1	AR 40	NI 65	GE 75	BR 89	SR 103	NB 111	RU 117	AG 113M	IN 123M
H 2	AR 41	NI 66	GE75M	BR 90	SR 104	NB 112	RU 118	AG 114	IN 124
H 3	AR 42	NI 72	GE 76	BR 91	Y 89	MO 92	RU 119	AG 115	IN 125
H 4	K 39	NI 73	GE 77	BR 92	Y 89M	MO93M	RU 120	AG 115M	IN 125M
HE 3	K 40	NI 74	GE77M	BR 93	Y 90	MO 93	RH 102	AG 116	IN 126
HE 4	K 41	NI 75	GE 78	BR 94	Y 90M	MO 94	RH 103	AG 116M	IN 127
HE 6	K 42	NI 76	GE 79	BR 95	Y 91	MO 95	RH103M	AG 117	IN 127M
LI 6	K 43	NI 77	GE 80	BR 96	Y 91M	MO 96	RH 104	AG 117M	IN 128
LI 7	K 44	NI 78	GE 81	KR 78	Y 92	MO 97	RH104M	AG 118	IN 129
LI 8	CA 40	CU 62	GE 82	KR 79	Y 93	MO 98	RH 105	AG 118M	IN 130
BE 8	CA 41	CU 63	GE 83	KR79M	Y 94	MO 99	RH105M	AG 119	IN 131
BE 9	CA 42	CU 64	GE 84	KR 80	Y 95	MO 100	RH 106	AG 120	IN 132
BE 10	CA 43	CU 65	GE 85	KR 81	Y 96	MO 101	RH106M	AG 121	IN 133
BE 11	CA 44	CU 66	GE 86	KR81M	Y 97	MO 102	RH 107	AG 122	IN 134
B 10	CA 45	CU 67	GE 87	KR 82	Y 98	MO 103	RH 108	AG 123	SN 112
B 11	CA 46	CU 72	GE 88	KR 83	Y 99	MO 104	RH108M	AG 124	SN 113
B 12	CA 47	CU 73	AS 75	KR83M	Y 100	MO 105	RH 109	AG 125	SN 113M
C 12	CA 48	CU 74	AS 76	KR 84	Y 101	MO 106	RH109M	AG 126	SN 114
C 13	CA 49	CU 75	AS 77	KR 85	Y 102	MO 107	RH 110	AG 127	SN 115
C 14	SC 45	CU 76	AS 78	KR85M	Y 103	MO 108	RH110M	AG 128	SN 116
C 15	SC 46	CU 77	AS 79	KR 86	Y 104	MO 109	RH 111	CD 106	SN 117
N 13	SC46M	CU 78	AS 80	KR 87	Y 105	MO 110	RH 112	CD 107	SN 117M
N 14	SC 47	CU 79	AS 81	KR 88	Y 106	MO 111	RH 113	CD 108	SN 118
N 15	SC 48	CU 80	AS 82	KR 89	Y 107	MO 112	RH 114	CD 109	SN 119
N 16	SC 49	CU 81	AS82M	KR 90	ZR 89	MO 113	RH 115	CD 110	SN 119M
O 16	SC 50	ZN 63	AS 83	KR 91	ZR 90	MO 114	RH 116	CD 111	SN 120
O 17	TI 46	ZN 64	AS 84	KR 92	ZR90M	MO 115	RH 117	CD 111M	SN 121
O 18	TI 47	ZN 65	AS 85	KR 93	ZR 91	TC 97	RH 118	CD 112	SN 121M
O 19	TI 48	ZN 66	AS 86	KR 94	ZR 92	TC 97M	RH 119	CD 113	SN 122
F 19	TI 49	ZN 67	AS 87	KR 95	ZR 93	TC 98	RH 120	CD 113M	SN 123
F 20	TI 50	ZN 68	AS 88	KR 96	ZR 94	TC 99	RH 121	CD 114	SN 123M
NE 20	TI 51	ZN 69	AS 89	KR 97	ZR 95	TC 99M	RH 122	CD 115	SN 124
NE 21	V 49	ZN69M	AS 90	KR 98	ZR 96	TC100	RH 123	CD 115M	SN 125
NE 22	V 50	ZN 70	SE 74	RB 85	ZR 97	TC101	PD 102	CD 116	SN 125M
NE 23	V 51	ZN 71	SE 75	RB 86	ZR 98	TC 102	PD 103	CD 117	SN 126
NA 22	V 52	ZN71M	SE 76	RB86M	ZR 99	TC102M	PD 104	CD 117M	SN 127
NA 23	V 53	ZN 72	SE 77	RB 87	ZR 100	TC 103	PD 105	CD 118	SN 127M
NA 24	V 54	ZN 73	SE77M	RB 88	ZR 101	TC 104	PD 106	CD 119	SN 128
NA24M	CR 50	ZN 74	SE 78	RB 89	ZR 102	TC 105	PD 107	CD 119M	SN 129
NA 25	CR 51	ZN 75	SE 79	RB 90	ZR 103	TC 106	PD107M	CD 120	SN 129M
MG 24	CR 52	ZN 76	SE79M	RB90M	ZR 104	TC 107	PD 108	CD 121	SN 130
MG 25	CR 53	ZN 77	SE 80	RB 91	ZR 105	TC 108	PD 109	CD 122	SN 131
MG 26	CR 54	ZN 78	SE 81	RB 92	ZR 106	TC 109	PD109M	CD 123	SN 132
MG 27	CR 55	ZN 79	SE81M	RB 93	ZR 107	TC 110	PD 110	CD 124	SN 133
MG 28	MN 54	ZN 80	SE 82	RB 94	ZR 108	TC 111	PD 111	CD 125	SN 134
AL 27	MN 55	ZN 81	SE 83	RB 95	ZR 109	TC 112	PD111M	CD 126	SN 135
AL 28	MN 56	ZN 82	SE83M	RB 96	NB 91	TC 113	PD 112	CD 127	SN 136
AL 29	MN 57	ZN 83	SE 84	RB 97	NB 92	TC 114	PD 113	CD 128	SB 121
AL 30	MN 58	GA 69	SE 85	RB 98	NB 93	TC 115	PD 114	CD 129	SB 122
SI 28	FE 54	GA 70	SE85M	RB 99	NB93M	TC 116	PD 115	CD 130	SB 122M
SI 29	FE 55	GA 71	SE 86	RB 100	NB 94	TC 117	PD 116	CD 131	SB 123
SI 30	FE 56	GA 72	SE 87	RB 101	NB94M	TC 118	PD 117	CD 132	SB 124
SI 31	FE 57	GA72M	SE 88	SR 84	NB 95	RU 96	PD 118	IN 113	SB 124M
SI 32	FE 58	GA 73	SE 89	SR 85	NB95M	RU 97	PD 119	IN 113M	SB 125
P 31	FE 59	GA 74	SE 90	SR85M	NB 96	RU 98	PD 120	IN 114	SB 126
P 32	CO 58	GA 75	SE 91	SR 86	NB 97	RU 99	PD 121	IN 114M	SB 126M
P 33	CO58M	GA 76	SE 92	SR 87	NB97M	RU 100	PD 122	IN 115	SB 127
P 34	CO 59	GA 77	SE 93	SR87M	NB 98	RU 101	PD 123	IN 115M	SB 128
S 32	CO 60	GA 78	BR 79	SR 88	NB98M	RU 102	PD 124	IN 116	SB 128M
S 33	CO60M	GA 79	BR79M	SR 89	NB 99	RU 103	PD 125	IN 116M	SB 129
S 34	CO 61	GA 80	BR 80	SR 90	NB99M	RU 104	PD 126	IN 117	SB 130
S 35	CO 62	GA 81	BR80M	SR 91	NB100	RU 105	AG 106	IN 117M	SB 130M
S 36	CO 72	GA 82	BR 81	SR 92	NB100M	RU 106	AG 107	IN 118	SB 131
S 37	CO 73	GA 83	BR 82	SR 93	NB 101	RU 107	AG 108	IN 119	SB 132
CL 35	CO 74	GA 84	BR82M	SR 94	NB 102	RU 108	AG108M	IN 119M	SB 132M
CL 36	CO 75	GA 85	BR 83	SR 95	NB 103	RU 109	AG 109	IN 120	SB 133
CL 37	NI 58	GE 70	BR 84	SR 96	NB 104	RU 110	AG109M	IN 120M	SB 134
CL 38	NI 59	GE 71	BR84M	SR 97	NB 105	RU 111	AG 110	IN 120M	SB 134M
CL38M	NI 60	GE71M	BR 85	SR 98	NB 106	RU 112	AG110M	IN 121	SB 135
AR 36	NI 61	GE 72	BR 86	SR 99	NB 107	RU 113	AG 111	IN 121M	SB 136

Table 2 (cont.): the 1312 nuclides included in the FORNAX XML default nuclear data.

SB 137	XE 125	BA 135	CE 153	PM 153	GD 159	YB 175M	IR 193	PO 211	NP 241
SB 138	XE 125M	BA 135M	CE 154	PM 154	GD 160	YB 176	IR 194	PO 211M	PU 236
SB 139	XE 126	BA 136	CE 155	PM 154M	GD 161	YB 177	IR 194M	PO 212	PU 237
TE 120	XE 127	BA 136M	CE 156	PM 155	GD 162	LU 175	PT 190	PO 213	PU 238
TE 121	XE 127M	BA 137	CE 157	PM 156	GD 163	LU 176	PT 191	PO 214	PU 239
TE 121M	XE 128	BA 137M	PR 139	PM 157	GD 164	LU 176M	PT 192	PO 215	PU 240
TE 122	XE 129	BA 138	PR 140	PM 158	GD 165	LU 177	PT 193	PO 216	PU 241
TE 123	XE 129M	BA 139	PR 141	PM 159	TB 157	LU 177M	PT 193M	PO 218	PU 242
TE 123M	XE 130	BA 140	PR 142	PM 160	TB 159	HF 174	PT 194	AT 217	PU 243
TE 124	XE 131	BA 141	PR 142M	PM 161	TB 160	HF 175	PT 195	RN 218	PU 244
TE 125	XE 131M	BA 142	PR 143	PM 162	TB 161	HF 176	PT 195M	RN 219	PU 245
TE 125M	XE 132	BA 143	PR 144	SM 144	TB 162	HF 177	PT 196	RN 220	PU 246
TE 126	XE 133	BA 144	PR 144M	SM 145	TB 162M	HF 178	PT 197	RN 222	AM 239
TE 127	XE 133M	BA 145	PR 145	SM 146	TB 163	HF 178M	PT 197M	FR 221	AM 240
TE 127M	XE 134	BA 146	PR 146	SM 147	TB 163M	HF 179	PT 198	FR 223	AM 241
TE 128	XE 135	BA 147	PR 147	SM 148	TB 164	HF 179M	PT 199	RA 222	AM 242M
TE 129	XE 135M	BA 148	PR 148	SM 149	TB 165	HF 180	PT 199M	RA 223	AM 242
TE 129M	XE 136	BA 149	PR 149	SM 150	DY 156	HF 180M	AU 197	RA 224	AM 243
TE 130	XE 137	BA 150	PR 150	SM 151	DY 157	HF 181	AU 198	RA 225	AM 244M
TE 131	XE 138	BA 151	PR 151	SM 152	DY 158	HF 182	AU 199	RA 226	AM 244
TE 131M	XE 139	BA 152	PR 152	SM 153	DY 159	TA 180	AU 200	RA 228	AM 245
TE 132	XE 140	LA 137	PR 153	SM 154	DY 160	TA 181	HG 196	AC 225	AM 246
TE 133	XE 141	LA 138	PR 154	SM 155	DY 161	TA 182	HG 197	AC 227	CM 241
TE 133M	XE 142	LA 139	PR 155	SM 156	DY 162	TA 182M	HG 197M	AC 228	CM 242
TE 134	XE 143	LA 140	PR 156	SM 157	DY 163	TA 183	HG 198	TH 226	CM 243
TE 135	XE 144	LA 141	PR 157	SM 158	DY 164	W 180	HG 199	TH 227	CM 244
TE 136	XE 145	LA 142	PR 158	SM 159	DY 165	W 181	HG 199M	TH 228	CM 245
TE 137	XE 146	LA 143	PR 159	SM 160	DY 165M	W 182	HG 200	TH 229	CM 246
TE 138	XE 147	LA 144	ND 141	SM 161	DY 166	W 183M	HG 201	TH 230	CM 247
TE 139	CS 131	LA 145	ND 142	SM 162	HO 163	W 183	HG 202	TH 231	CM 248
TE 140	CS 132	LA 146	ND 143	SM 163	HO 165	W 184	HG 203	TH 232	CM 249
TE 141	CS 133	LA 147	ND 144	SM 164	HO 166	W 185	HG 204	TH 233	CM 250
TE 142	CS 134	LA 148	ND 145	SM 165	HO 166M	W 185M	HG 205	TH 234	CM 251
I 125	CS 134M	LA 149	ND 146	EU 149	ER 162	W 186	TL 203	PA 231	BK 249
I 126	CS 135	LA 150	ND 147	EU 150	ER 163	W 187	TL 204	PA 232	BK 250
I 127	CS 135M	LA 151	ND 148	EU 151	ER 164	W 188	TL 205	PA 233	BK 251
I 128	CS 136	LA 152	ND 149	EU 152	ER 165	W 189	TL 206	PA 234M	CF 249
I 129	CS 137	LA 153	ND 150	EU 152M	ER 166	RE 185	TL 207	PA 234	CF 250
I 130	CS 138	LA 154	ND 151	EU 153	ER 167	RE 186	TL 208	PA 235	CF 251
I 130M	CS 138M	LA 155	ND 152	EU 154	ER 167M	RE 187	TL 209	U 230	CF 252
I 131	CS 139	CE 136	ND 153	EU 155	ER 168	RE 188	PB 204	U 231	CF 253
I 132	CS 140	CE 137	ND 154	EU 156	ER 169	RE 188M	PB 205	U 232	CF 254
I 133	CS 141	CE 137M	ND 155	EU 157	ER 170	RE 189	PB 206	U 233	CF 255
I 133M	CS 142	CE 138	ND 156	EU 158	ER 171	OS 184	PB 207	U 234	ES 253
I 134	CS 143	CE 139	ND 157	EU 159	ER 172	OS 185	PB 208	U 235	ES 254M
I 134M	CS 144	CE 139M	ND 158	EU 160	TM 169	OS 186	PB 209	U 236	ES 254
I 135	CS 145	CE 140	ND 159	EU 161	TM 170	OS 187	PB 210	U 237	ES 255
I 136	CS 146	CE 141	ND 160	EU 162	TM 170M	OS 188	PB 211	U 238	
I 136M	CS 147	CE 142	ND 161	EU 163	TM 171	OS 189	PB 212	U 239	Transpire
I 137	CS 148	CE 143	PM 145	EU 164	TM 172	OS 190	PB 214	U 240	
I 138	CS 149	CE 144	PM 146	EU 165	TM 173	OS 190M	BI 208	U 241	CO57
I 139	CS 150	CE 145	PM 147	GD 152	YB 168	OS 191	BI 209	NP 235	NI57
I 140	BA 130	CE 146	PM 148	GD 153	YB 169	OS 191M	BI 210	NP 236M	EU 152N
I 141	BA 131	CE 147	PM 148M	GD 154	YB 170	OS 192	BI 210M	NP 236	EU 154M
I 142	BA 131M	CE 148	PM 149	GD 155	YB 171	OS 193	BI 211	NP 237	AU 196
I 143	BA 132	CE 149	PM 150	GD 155M	YB 172	OS 194	BI 212	NP 238	AU 196M
I 144	BA 133	CE 150	PM 151	GD 156	YB 173	IR 191	BI 213	NP 239	AU 196N
I 145	BA 133M	CE 151	PM 152	GD 157	YB 174	IR 192	BI 214	NP 240M	
XE 124	BA 134	CE 152	PM 152M	GD 158	YB 175	IR 192M	PO 210	NP 240	

Figures 4 and 5 are plots of the average gamma energy per decay and half-life, respectively, of those 1198 missing nuclides. Figure 6 is a plot of a “decay dose factor” for those same 1198 nuclides. The decay dose factor is computed by folding the average gamma energy per decay with appropriate gamma-to-dose conversion factors, and provides an estimation of the gamma dose associated with the decay of nuclide. The decay dose factors have units of dose rate per unit flux; those in Figure 6 were calculated using EAF 2007 average gamma energy data and ANSI-ANS-1991 gamma-to-dose conversion coefficients, [12]; Figure 7 is a plot of the aforementioned coefficients.

Table 3: comparison of FORNAX and EAF 2007 decay data (half-life and average gamma energy) for the 27 nuclides having decay gamma spectrum in the XML file.

nuclide name	In ORIGEN-S?	FORNAX half-life (s)	FORNAX Eg (MeV)	EAF-2007 half-life (s)	EAF-2007 Eg (MeV)	half-life ratio	Eg ratio
Au-196	No	5.86E+05	0.47	5.34E+05	0.47	1.10	1.00
Au-196m	No	8.10E+00	0.08	8.10E+00	0.00	1.00	28.61
Au-196n	No	3.46E+04	0.23	3.46E+04	0.24	1.00	0.98
Ca-47	Yes	3.92E+05	1.05	3.92E+05	1.06	1.00	0.99
Co-57	No	2.34E+07	0.12	2.35E+07	0.13	1.00	0.96
Co-58	Yes	6.13E+06	0.98	6.12E+06	0.98	1.00	1.00
Co-58m	Yes	3.29E+04	0.00	3.20E+04	0.00	1.03	1.04
Co-60	Yes	1.66E+08	2.50	1.66E+08	2.50	1.00	1.00
Cr-51	Yes	2.39E+06	0.03	2.39E+06	0.03	1.00	1.02
Cs-134	Yes	6.51E+07	1.55	6.52E+07	1.56	1.00	1.00
Cs-134m	Yes	1.05E+04	0.03	1.05E+04	0.03	1.00	0.98
Eu-152	Yes	4.21E+08	1.16	4.27E+08	1.16	0.99	1.00
Eu-152m	Yes	3.36E+04	0.30	3.34E+04	0.31	1.00	0.97
Eu-152n	No	5.76E+03	0.14	5.76E+03	0.08	1.00	1.85
Eu-154	Yes	2.71E+08	1.25	2.71E+08	1.25	1.00	1.01
Eu-154m	No	2.76E+03	0.15	2.78E+03	0.07	0.99	2.02
Fe-59	Yes	3.85E+06	1.19	3.84E+06	1.19	1.00	1.00
K-40	Yes	4.03E+16	0.16	3.99E+16	0.16	1.01	1.00
Mn-54	Yes	2.70E+07	0.84	2.70E+07	0.84	1.00	1.00
Mn-56	Yes	9.28E+03	1.69	9.30E+03	1.71	1.00	0.99
Mo-99	Yes	2.37E+05	0.27	2.37E+05	0.15	1.00	1.83
N-16	Yes	7.13E+00	4.49	7.13E+00	4.62	1.00	0.97
Na-22	Yes	8.21E+07	2.19	8.21E+07	2.19	1.00	1.00
Na-24	Yes	5.28E+04	4.13	5.38E+04	4.12	0.98	1.00
Na-24m	Yes	2.02E-02	0.47	2.00E-02	0.47	1.01	1.00
Ni-57	No	1.30E+05	1.38	1.29E+05	1.94	1.01	0.71
Zn-65	Yes	2.11E+07	0.58	2.11E+07	0.58	1.00	1.00

At the time of writing, only 27 of the 1312 nuclides in the FORNAX XML file had decay gamma spectrum information implemented. These nuclides are listed in Table 3, and the XML decay constants and average gamma energy per decay compared with those of the EAF 2007 libraries. Values compare well, the only noticeable discrepancies being those of Au-196m, Eu-152n, Eu-154m and Mo-99 decay gamma energies. The reason for some of these differences, and more details of the quality of the decay gamma data in the XML file, are given in following sections of this document.

IV. 1D TEST PROBLEM

The geometry chosen for a first, preliminary comparison of these tools was purposely chosen to be simple, in order to focus the problem in analysing the performance of two such different algorithms and on the important issue of the nuclear data quality and adequacy. A set of six 20x20x10 cm slabs with reflecting planes around them provided an essentially 1D problem of adjacent infinite slabs of equal thickness, as in Figure 8. As for the materials, steel and water were alternated to provide both moderation and attenuation and thus different neutron spectra properties along the geometry. Air slabs were located at the front and rear to provide source and dose tallying volumes; steel composition is shown in Table 4. Natural isotopic abundances were used throughout. The neutron source was located in the front air slab, consisting of isotropic, mono-energetic, 14.1 MeV neutrons at an intensity of 3×10^{11} n/cc.s, typical of a volume-averaged ITER plasma. The irradiation history also tried to simulate ITER conditions, consisting of a one year period at 5% load factor (representing the fluence of approximately $2,500 \times 10^7$ ITER pulses) immediately followed by a single 10' pulse at 100% power. This scheme should generate both short and long-lived activation at similar rates as those found in ITER.

Isotopic production and activation gamma sources were computed using both codes at four different decay times following irradiation: 1 hour, 1 day, 10 days and 1 year. These were used in photon runs with MCNP and ATTILA to ascertain and compare the shutdown dose throughout the geometry at those same times. Neutron runs were performed using FENDL 2.1 libraries in both MCNP and ATTILA, and results binned in the 175-group VITAMIN-J fusion standard energy format in both cases; the same one used by ATTILA for neutron transport. Activation was calculated also in this format using the EAF-2007 activation libraries with FISPACT, [6], and using combined FENDL 2.1 and FORNAX XML data with ATTILA. Activation gamma sources were produced in the 24-group FISPACT format for MCNP, and in the default 42-group ATTILA format for this code. Photon runs were performed using FENDL 2.1 data in both cases. The spatial resolution of the MCNP mesh tallies was chosen to be 1cm, and an importance map implemented for variance reduction, in order to achieve good statistics. ATTILA mesh size was also 1cm, and the following solver options were employed: TCL quadrature, S_N order 8, P_N order 2 and convergence criterion 0.01%.

Table 4: steel composition (%wt, Fe balance).

C	0.8	Co	0.1
Si	1.0	Ni	12.0
Cr	17.0	Cu	0.2
Mn	2.0	Mo	2.5

V. RESULTS AND ANALYSIS

As expected from earlier comparison exercises between MCNP and ATTILA, neutron transport results for both codes compare extremely well. Figure 9 shows the total neutron flux profiles resulting from the neutron runs of MCNP and ATTILA; MCNP data are integrated over mesh tally voxel, whereas ATTILA data are point-wise flux interrogations. Results are within 3% at all locations. Comparison of the neutron spectra integrated over the volume of slabs SS1 and SS3 (first and last steel ones) are shown in Figure 10.

FISPACT contact dose rate data were used as a guideline to compare isotopic production from the activation runs on meaningful isotopes. According to these, the dominant nuclides responsible for the vast majority of the shutdown dose at the times of interest were Mn-56, Ni-57, Mo-99, Cr-51, Fe-59, Co-58, Mn-54 and Co-60. Contributions of each one vary greatly with decay time and location (i.e. neutron spectra); Tables 5 illustrates these for SS1 and SS3. Figure 11 shows the ratio of ATTILA to MCNP production of the above isotopes in the three steel slabs. Results are all within 25% except for Cr-51 and Mo-99. Analysis of the FORNAX data of ATTILA and comparison with EAF data revealed the reasons for the relatively larger discrepancies in these nuclides: for Cr-51 a large difference was found in the Cr-52(n,2n) and Cr-50(n,g) pathway cross section values between the two libraries; for Mo-99 it was the absence of Mo-100(n,2n) cross section information in the FORNAX data. ATTILA isotopic production results also revealed the absence of a large number of isotopes produced by FISPACT and the EAF libraries, all of which had negligible contribution to the dose field, due to their absence or the absence of their pathway reactions in the FORNAX XML library.

FORNAX and EAF decay and gamma line data for the above dominant nuclides were compared and found to match well, as illustrated in Figures 12 – 18: decay constants within 1%, gamma line energies within 2% and intensities within 5%; therefore most differences in decay photon source between the codes can be related to those in isotopic production. The only exceptions to this rule are:

Table 5: SS1 and SS3 FISPACT contact dose dominant nuclide contributions (%) and pathways at different decay times.

nuclide	half-life	1h SS1	1d SS1	10d SS1	1y SS1	1h SS3	1d SS3	10d SS3	1y SS3	reaction pathways
Mn-56	2.58h	76.5	0.7			93.3				Mn-55(n,g)
Ni-57	35.9h	1.5	4.4							Ni-58(n,2n); Fe-56(n,p)
Mo-99	2.75d	0.1	0.4							Mo-100(n,2n); Mo-98(n,g)
Cr-51	27.7d	0.4	1.5	1.4		0.3	4.7			Cr-50(n,g); Cr-52(n,2n)
Fe-59	44.5d					0.4	5.4	5.2		Fe-58(n,g); Ni-58(n,p)
Co-58	71.0d	13.6	59.7	61.9	9.8	3.4	46.4	47.5	4.5	Co-59(n,p)
Mn-54	312d	6.2	27.3	30.3	70.3	0.9	13.4	14.7	20.5	Mn-55(n,2n)
Co-60	5.27y		3.0	3.4	15.2	1.6	24.5	27.5	74.0	Co-59(n,g)

- the absence of a high number of low-energy lines (X-rays) from the FORNAX data, compared with EAF libraries;
- the absence from the FORNAX data of 511 keV lines corresponding to electron-positron annihilation photons which occur in some nuclides following beta decay (e.g. Ni-57 and Co-58 in this case);
- an extra 141 keV line in Mo-99 has also been observed in the XML file; this line corresponds in fact to Tc-99m, and is responsible for the significant difference in average gamma energy found for this nuclide.

MCNP and ATTILA activation source strength profiles and spectra for the four decay times of interest are shown in Figures 19 – 26. The presence of all those low-energy lines in the EAF data, largely unimportant for dose analysis, is noticeable in both the profiles and spectra. They make the FISPACT profiles look artificially larger than the ATTILA ones; when these photons are not accounted for (yellow points) MC-R2S and ATTILA profiles are much closer.

Results of the photon runs for the above activation sources are illustrated in Figures 27 – 32 in which total photon flux profiles and spectra at the some of the locations and decay times of interest are shown. Photon spectra are the outcome of the decay gamma source transport, which results in a combination of unscattered photons, pair production depletion, positron annihilation production and Compton continua. Photon spectra match better at high energies, due to the aforementioned large number of low energy source photons in the EAF libraries.

Finally, photon spectra data at the front and rear air slabs were used to compute dose rates using again ANSI-ANS-1991 gamma-flux-to-dose conversion factors, [12]; results are summarised in Figures 33 and 34, and in Table 6. At all decay times and locations, total dose values are within 15% of each other. As expected, low energy lines contribution to the dose is insignificant, as determined by the conversion factors, and it is the high energy photons that dominate the dose (i.e. larger area under curves in the Figures). Since these compare well in both codes it is not surprising that absolute dose values are similar.

Table 6: R2S total decay dose results for test problem (mSv/h).

location	front air	front air	rear air	rear air
decay time	ATTILA-ASG	MC-R2S	ATTILA-ASG	MC-R2S
1 hour	62,000	67,000	134	150
1 day	14,600	14,400	11.0	9.7
10 days	13,000	13,600	9.8	8.3
1 year	2,500	2,800	2.5	3.0

VI. IMPROVEMENT OF ATTLA ACTIVATION DATA

The fact that ATTLA and MC-R2S results are so similar indicates that the default FORNAX XML data is adequate to calculate activation dose for the simple materials and irradiation history of this problem. Dominant isotopes, precursors, reaction pathway and decay information (cross section, decay constants, gamma line energy and intensity) seem sufficient for the undemanding conditions of this test problem. Even so, formalisation of the validity of FORNAX data for activation analysis in generic fusion conditions, and particularly for a much wider range of elements, can only be achieved through the implementation of certified decay gamma line data for a larger range of nuclides than the current 27 ones in the XML file. Moreover, reaction pathways for the generation of these nuclides also require careful consideration.

In order to be able to quickly and efficiently assess the required data, identification of the dominant contributors to the decay gamma dose of naturally-occurring elements is a fundamental first step. In principle, this might seem a cumbersome task: the contribution of any given nuclide to the dose field is highly problem-dependent, complexly varying with neutron energy, material and geometry details. Any generalisation inevitably introduces uncertainty in the validity of the results.

A coarse but nonetheless insightful evaluation can be made through the review of generic activation properties of elements in available documentation. In reference [13], the most important activation properties of all natural elements up to uranium are evaluated, summarised and reported. Dominant nuclides, precursors and reaction pathways for several radiological quantities (activity, decay heat, contact dose rate, etc) are analysed in a comprehensive manner using fusion-relevant neutron spectra and EAF nuclear data. Through the use of the powerful importance diagram technique, [14], a total of 754 nuclides are reported as primary (>50%) and secondary (<50% but >1%) contributors to those radiological quantities at some point in a neutron energy – decay time phase space. A list of these nuclides, their precursors and pathway reactions can be found in the same reference. For the FORNAX data to produce activation results at similar levels of accuracy and reliability as those provided by the EAF data, implementation of complete nuclear data for all those 754 nuclides should be considered: decay constants, branching ratios, gamma spectra and pathway reaction cross-sections. Of these 754 dominant nuclides, 221 are not currently implemented in FORNAX XML; of the 533 which are, only the 27 previously listed have gamma line data.

The main purpose of FORNAX is, however, the calculation of activation gamma sources of relevance to fusion machines, and particularly to ITER maintenance for the time being. Bearing this in mind, a finer search of nuclide requirements can be performed by looking at more specific information on dominant nuclides and reactions. In particular, the contact dose information at the time scale of ITER maintenance operations can be used, e.g. between 1 hour and 1 year. Whilst not being able to accurately predict the decay gamma dose in an intricate problem (see example in Appendix 3), the contact dose approximation in FISPACT provides a discerning estimation of the relative importance of gamma lines and responsible nuclides in the activation dose.

Analysis of such data in reference [13] reveals that only 145 of the 754 EAF dominant nuclides have primary or secondary (i.e. >1%) contributions to the contact dose within the above time scale; Table 7 lists these 145 nuclides and their elemental precursors. Note that only 28 of those 145 are not currently implemented at all in the FORNAX XML file. Of the 117 which are, 18 have decay gamma line data. Figures 35 and 36 plot the half-lives and average gamma energy per decay of these 145 nuclides, comparing them with those of all the 2231 EAF 2007 nuclides.

Table 7: EAF contact dose dominant contributors between 1 hour and 1 year decay time.

nuclide	FORNAX?	precursors	nuclide	FORNAX?	precursors
Be-10	YES	B, C, N, O, F	Te-131m	YES	Te
Na-22	YES	Ne, Na, Mg, Al, Si, P, S	Te-127	YES	Te, I
Na-24	YES	Ne, Na, Mg, Al, Si, P	Te-123m	YES	Te
Al-26	NO	Al, Si, P	Te-121m	YES	Te
P-32	YES	P, S, Cl, Ar	I-126	YES	Te, I
Cl-36	YES	Cl	I-130	YES	Te
Ar-37	YES	Ar,	I-131	YES	Te
Ar-39	YES	Ar, K	I-132	YES	Th, U
K-42	YES	Ar, K	Xe-127	YES	Te, I, Xe
Ca-47	YES	Ca	Cs-132	YES	Xe, Cs, Ba
Sc-46	YES	Sc, Ti, V, Cr	Cs-134	YES	Xe, Cs, Ba, La, Th, U
Sc-47	YES	Ca	Cs-136	YES	Xe, Cs, Ba, Th, U
Sc-44	NO	Sc	Ba-131	YES	Ba
Sc-48	YES	Ti, V, Cr	Ba-133	YES	Ba
V-49	YES	V, Cr	Ba-135m	YES	Ba
Cr-51	YES	Cr	Ba-137m	YES	Ba, Th, U
Mn-54	YES	Cr, Mn, Fe	La-140	YES	Ba, La, Ce, Pr, Th, U
Fe-55	YES	Fe	Ce-139	YES	La, Ce, Pr
Fe-59	YES	Fe, Ni	Ce-141	YES	Ce
Co-60	YES	Fe, Co, Ni, Cu	Pr-142	YES	Pr
Co-58	YES	Co, Ni	Pr-144	YES	Th, U
Co-57	YES	Ni	Pm-148	YES	Nd, Th, U
Ni-57	YES	Ni	Pm-148m	YES	Nd, Th, U
Cu-64	YES	Cu,	Pm-151	YES	Nd
Zn-65	YES	Cu, Zn, Ga, Ge	Nd-147	YES	Nd
Ga-72	YES	Ga, Ge	Eu-152	YES	Nd, Eu
Ge-69	NO	Ga, Ge	Eu-154	YES	Nd, Sm, Eu, Gd, Th, U
Ge-71	YES	Ge	Eu-156	YES	Nd, Sm, Eu, Gd
As-74	NO	Ge, As, Se	Tb-158	NO	Dy
As-76	YES	Ge, As, Se	Tb-160	YES	Gd, Tb, Dy
Se-75	YES	As, Se, Br	Ho-166	YES	Dy, Ho
Br-82	YES	Se, Br, Kr	Ho-166m	YES	Dy, Ho
Kr-85	YES	Br, Kr, Rb	Tm-168	NO	Dy, Ho, Er, Tm, Yb
Kr-79	YES	Kr	Tm-170	YES	Ho, Er, Tm
Rb-84	NO	Kr, Rb, Sr	Tm-172	YES	Ho, Er, Tm, Yb
Rb-86	YES	Kr, Rb, Sr	Yb-169	YES	Tm, Yb
Rb-83	NO	Rb, Sr	Yb-175	YES	Yb
Sr-85	YES	Rb, Sr	Ta-182	YES	Yb, Lu, Hf, Ta, W
Y-88	NO	Sr, Y, Zr, Mo	Hf-175	YES	Yb, Lu
Y-89m	YES	Zr, Mo	Hf-181	YES	Lu, Hf
Zr-95	YES	Zr, Th, U	Hf-178m	YES	Yb, Lu
Zr-89m	NO	Zr, Mo	Hf-178n	NO	Yb, Lu
Nb-95	YES	Zr, Nb, Mo, Th, U	Hf-179n	NO	Yb, Lu
Nb-92m	NO	Nb, Mo	Lu-174	NO	Yb, Lu
Nb-94	YES	Nb, Mo	Lu-177	YES	Yb, Lu
Nb-96	YES	Mo	W-187	YES	W, Re
Nb-91m	NO	Mo	Re-184	NO	W, Re
Mo-99	YES	Mo	Re-184m	NO	Re
Ru-97	YES	Ru	Re-186	YES	W, Re
Ru-103	YES	Ru, Rh	Re-188	YES	W, Re
Rh-102	YES	Ru, Rh	Os-185	YES	W, Re, Os
Rh-102m	NO	Ru, Rh, Pd	Ir-190	NO	Re, Os, Ir
Rh-106	YES	U	Ir-192	YES	Re, Os, Ir, Pt
Tc-96	NO	Ru	Ir-194	YES	Ir
Ag-110m	YES	Pd, Ag, Cd, In	Ir-194m	YES	Ir, Pt, Au
Ag-106m	NO	Ag, Cd	Pt-191	YES	Ir
Ag-105	NO	Cd	Pt-193	YES	Ir, Pt
Cd-115	YES	Cd	Pt-195m	YES	Pt
Cd-115m	YES	Cd	Au-195	NO	Au, Hg
In-115m	YES	Cd	Au-196	YES	Pt, Au, Hg
In-113m	YES	In, Sn	Au-198	YES	Pt, Au, Hg
In-114	YES	In	Au-199	YES	Pt
In-114m	YES	In	Hg-203	YES	Hg, Pb
Sn-117m	YES	In, Sn	Tl-202	NO	Hg, Tl, Pb
Sb-120m	NO	Sn, Sb	Tl-204	YES	Hg, Tl, Pb
Sb-122	YES	Sn, Sb, Te	Tl-208	YES	Th, U
Sb-124	YES	Sn, Sb, Te, I	Pb-203	NO	Tl, Pb
Sb-125	YES	Sn, Sb, I	Bi-206	NO	Bi
Sb-126	YES	Sb	Bi-207	NO	Pb, Bi
Te-121	YES	Sb, Te	Bi-208	YES	Pb
Te-129	YES	Te	Pa-232	YES	Th, U
Te-129m	YES	Te			

VII. DISCUSSION

Two different tools for the estimation of activation dose in ITER and fusion devices based on the rigorous-two-step formalism are now available and have been described. The tools are based on the two main numerical methods used in radiation transport applications: Monte Carlo and discrete ordinates. They couple neutron, activation and photon calculations in an integrated manner, allowing for the fine spatial resolution required for this kind of analyses. A preliminary comparison in a simple, one-dimensional geometry and irradiation conditions has revealed that, despite differences in input nuclear data and output isotopic production and photon source, activation dose results at all decay times and locations of interest are within 15% of each other. Results serve as a first evaluation of the robustness and reliability of these tools for the estimation of shutdown doses in ITER. Given the simplicity of the test geometry, and particularly due to the fact that the MCNP mesh tally covered exactly the entire spatial domain, it can be argued that MC-R2S analyses and results conform to the standards of earlier MCNP, FISPACT and EAF data benchmarks for fusion applications, [15]. The fact that ATTILA and MC-R2S results are so similar indicates that, for the materials and irradiation history of this problem, the default FORNAX XML data is adequate for the calculation of activation dose. Dominant isotopes, precursors, reactions and decay information seem sufficient under the undemanding conditions of this test.

Even so, formalisation of the validity of FORNAX data for activation analysis in generic fusion conditions, i.e. a wider range of elements, can only be achieved through the implementation of certified decay gamma line data for a much larger range of nuclides than currently available. Implementation of data for nuclides not currently included in the FORNAX file might be necessary. Identification of the differences between EAF and FORNAX data, and of dominant contributors to the gamma dose of naturally-occurring elements, are two important first steps enabling fast and efficient assessment of data requirements. The evaluation and comparison of FORNAX and EAF data made here has revealed the following:

- Out of a total of 2231 nuclides in the EAF 2007 library, 1198 have been identified as having no counterpart in ATTILA data. A total of 1032 common nuclides have also been identified, and comparison of decay constants made. Only 27 FORNAX nuclides have currently implemented decay gamma spectra, which generally show good agreement with EAF data.
- Out of 1484 reaction cross sections in ATTILA data, 980 are described in the FORNAX XML file which currently allows for a 3-group description only; EAF uses a 175-group structure by default in more than 65,000 reactions.
- A review of literature on general activation properties using EAF data has shown 754 primary and secondary dominant nuclides for a range of radiological quantities (activity, contact dose, decay heat rates) in all naturally-occurring elements. Of these, 221 are not found in FORNAX XML.
- Only 145 of those 754 nuclides are found to contribute more than 1% to the contact dose rate of naturally-occurring elements within the time scale of ITER maintenance operations under generic fusion conditions. Of these 145, 117 already exist in FORNAX XML, 18 of which have decay gamma line data; 28 are not included at all.

It is recommended that implementation in the XML file of complete nuclear data (decay constants, branching ratios, decay gamma lines and pathway reaction cross-sections) for a much wider range of nuclides is made before ITER-related analyses are performed using the ATTILA ASG software. In particular, it is desirable to implement cross-section data in higher energy resolution, e.g. the 175 energy groups used by the EAF library. The information presented here can be used as a guideline for this implementation, which, if necessary, could be made in stages: first, and more urgently, the 145 nuclides which are dose-dominant at

ITER-relevant time scales; later the full 754 dominant at other times and/or to other radiological quantities.

A few QA considerations are also in place. ATTILA has undergone several benchmark exercises of its neutron and photon transport capabilities. The ASG module is currently also undergoing a benchmark study based on the “FNG shutdown dose experiment” recommended by the NEA, [5]. If successful, ATTILA will be in a position to fulfil ITER QA requirements; preliminary results are positive and seem to confirm the findings reported here. Although MCNP and FISPACT are two well-established and benchmarked codes for shutdown dose analyses in fusion applications, the novel mesh-tally implementation and activation source definition of MC-R2S are innovative and require at least a minimum benchmark in a full 3D, fusion-relevant geometry to guarantee their validity and comply with ITER QA. The comparison presented here is a first step in the right direction; eventually, the same NEA recommended exercise used to test ATTILA’s ASG seems the obvious choice.

The R2S method implemented in ATTILA and MC-R2S supersedes earlier approximations such as the semi-infinite slab contact dose available in FISPACT. An example of the differences between the R2S method and the semi-infinite slab approximation, based on the study presented here, is given in Appendix 3.

ACKNOWLEDGEMENTS

The authors would like to thank Greg Failla and Ian Davis of Transpire Inc. for their valuable help in producing this work and report. This work was funded jointly by the United Kingdom Engineering and Physical Sciences Research Council and by the European Communities under the contract of Association between EURATOM and UKAEA. The views and opinions expressed herein do not necessarily reflect those of the European Commission.

REFERENCES

- [1] X5 Monte Carlo Team, “MCNP – a general Monte Carlo N-Particle transport code: version5 user’s guide”, LANL report LA-CP-03-0245, October 2005.
- [2] T. Wareing et al., “ATTILA V5 user manual”, Transpire Inc., January 2006.
- [3] R.A. Forrest et al., “FISPACT 2007 user manual”, UKAEA **FUS 534**, March 2007.
- [4] Y. Chen et al., “Rigorous MCNP based shutdown dose rate calculations: computational scheme, verification calculations and applications to ITER”, *Fus. Eng. and Des.*, **63–64** (2002), p107.
- [5] M.Z. Youssef et al., “Benchmarking ATTILA using the FNG experiment on shutdown dose rate”, presented at the 4th ITER neutronics workshop, Cadarache, May 2006 (to be presented at the 18th TOFE conference, San Francisco, October 2008).
- [6] R.A. Forrest et al., “EAF 2007 neutron-induced cross section library”, UKAEA **FUS 535**, March 2007.
- [7] R. Pampin et al., “Evaluation of a 3D discrete ordinates radiation transport tool for support of ITER design”, *Fus. Eng. and Des.* **82** (2007) p2008.
- [8] M.Z. Youssef et al., “Comparing the prediction of ATTILA code to the experimental data of fusion integral experiments and to the results of MCNP code”, *Fus. Sci. and Tech.* **52** (2007) p801.
- [9] M.Z. Youssef et al., “Benchmarking ATTILA with ITER MCNP CAD Model”, Proc. 8th International Symposium on Fusion Nuclear Technology ISFNT-8, Heidelberg, October 2007 (to appear in *Fus. Eng. and Des.*).

- [10] J.C. Ryman et al., "ORIGEN-S data libraries", ORNL report, ORNL/NUREG/CSD-2/V3/R6, March 2000.
- [11] O.W. Hermann et al., "ORIGEN-S decay data library and half-life uncertainties", ORNL report, ORNL/TM-13624, September 1998.
- [12] American Nuclear Society, "Neutron and gamma-ray fluence-to-dose factors", ANS standard, ANSI/ANS-6.1.1-1991.
- [13] M.R. Gilbert et al., "Handbook of activation data calculated using EAF-2003", UKAEA **FUS 509**, July 2004.
- [14] R. A. Forrest, "Importance diagrams: a novel presentation of the response of a material to neutron irradiation", *Fus. Eng. and Des.* **43** (1998), p209.
- [15] Y. Chen et al., "Measurement and analysis of dose rates and gamma-ray fluxes in an ITER-shutdown dose rate experiment", *Fus. Eng. and Des.* **63-64** (2002), p213.

FIGURES

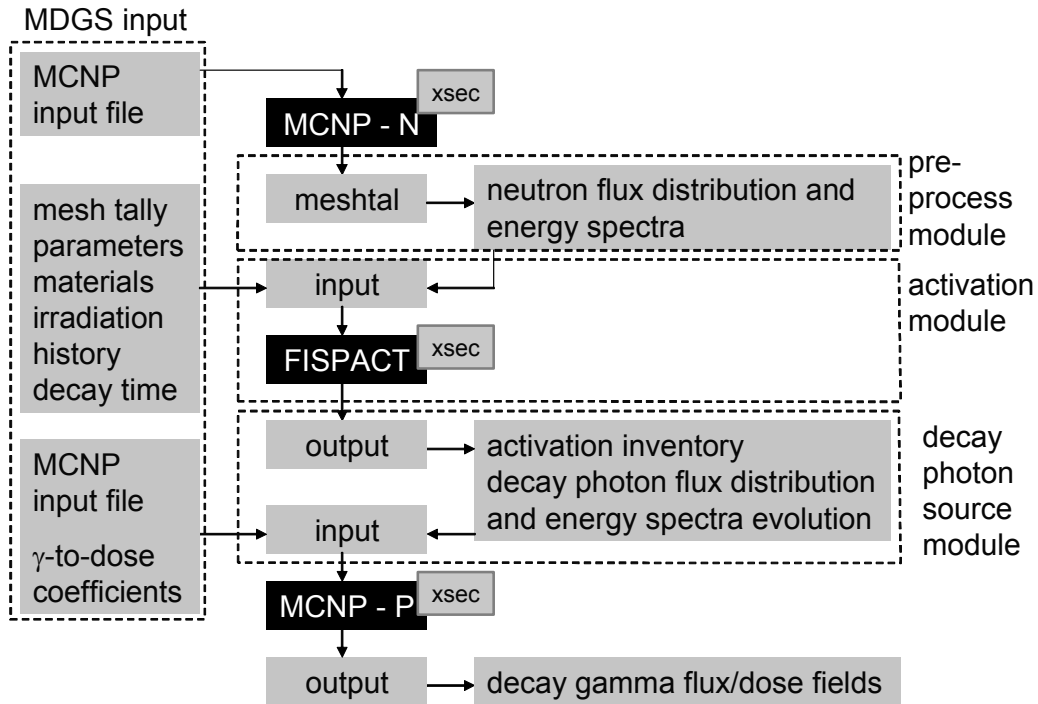


Fig. 1: MC-R2S flow chart.

```

- <nuclide id="02706000">
  <name>Co60</name>
  - <cross-sections energy="thermal" units="bn/atom">
    <ng>2</ng>
  </cross-sections>
  - <cross-sections energy="resonance" units="bn/atom">
    <ng>4.3</ng>
  </cross-sections>
  - <decay-data>
    <half-life units="s">1.663e+08</half-life>
    - <decay-mode name="beta-" fraction="1">
      - <spectrum emission="gamma" units="keV">
        <yield energy="347.14">0.000075</yield>
        <yield energy="826.1">0.000076</yield>
        <yield energy="1173.228">0.9985</yield>
        <yield energy="1332.492">0.999826</yield>
        <yield energy="2158.57">0.0000122</yield>
      </spectrum>
    </decay-mode>
  </decay-data>
</nuclide>
    
```

Fig. 2: FORNAX XML nuclear data library decay chain file notes for Co-60 nuclide.

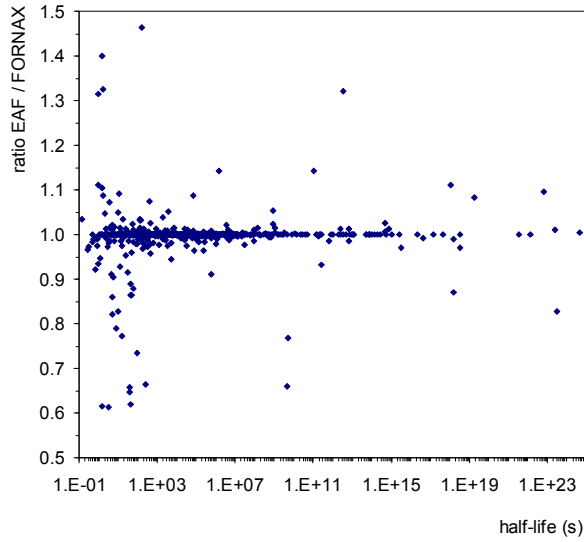


Fig. 3: ratio of EAF to FORNAX half-life values for 1032 common nuclides.

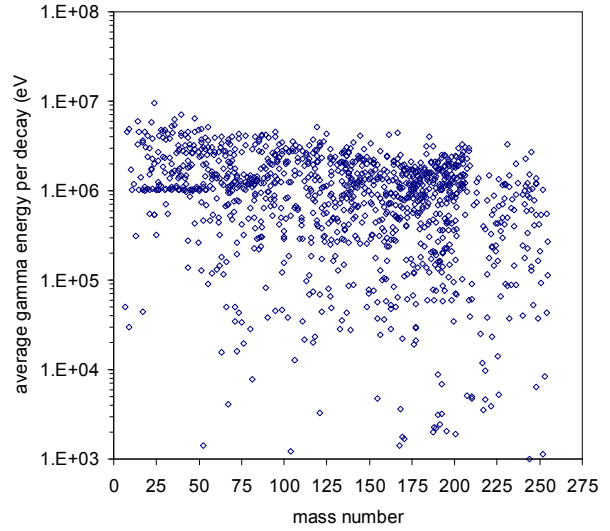


Fig. 4: average gamma energy per decay (eV) for 1198 EAF nuclides missing in FORNAX.

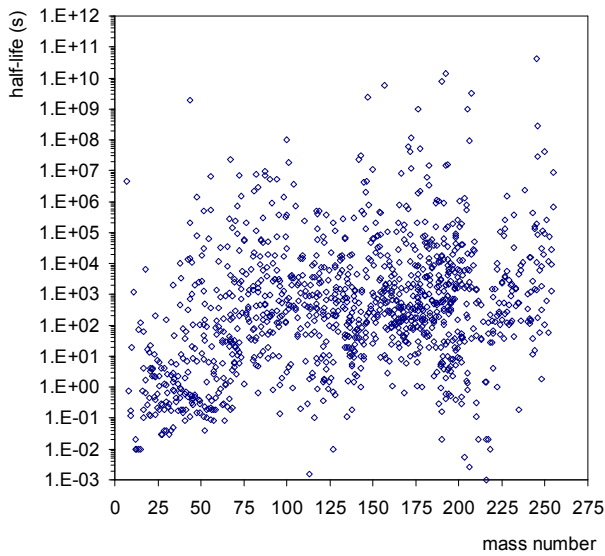


Fig. 5: half-life (s) for 1198 EAF nuclides missing in FORNAX.

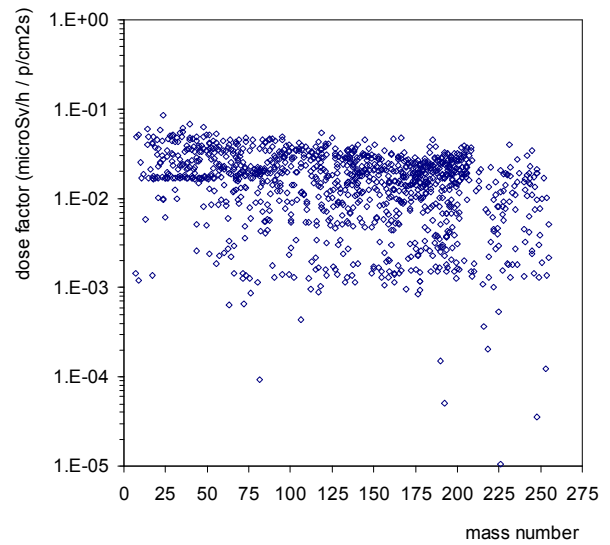


Fig. 6: decay dose factor ($\mu\text{Sv/h per } \gamma/\text{cm}^2\text{s}$) for 1198 EAF nuclides missing in FORNAX, calculated using ANSI-ANS-1991 factors.

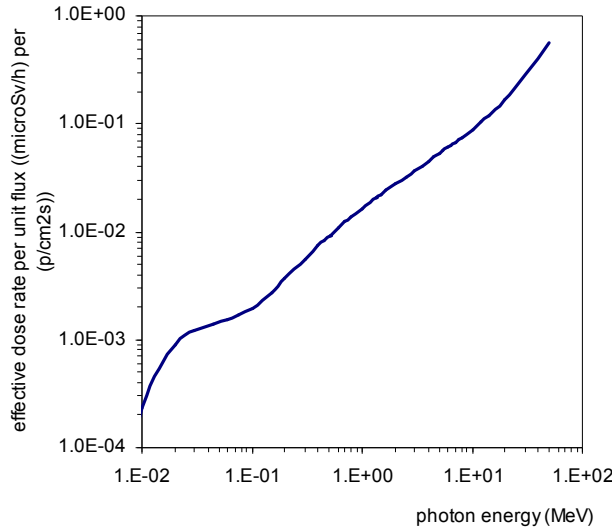


Fig. 7: ANSI-ANS-1991 gamma-to-dose conversion factors.

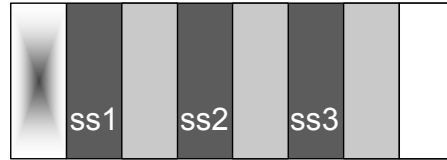


Fig. 8: test problem geometry.

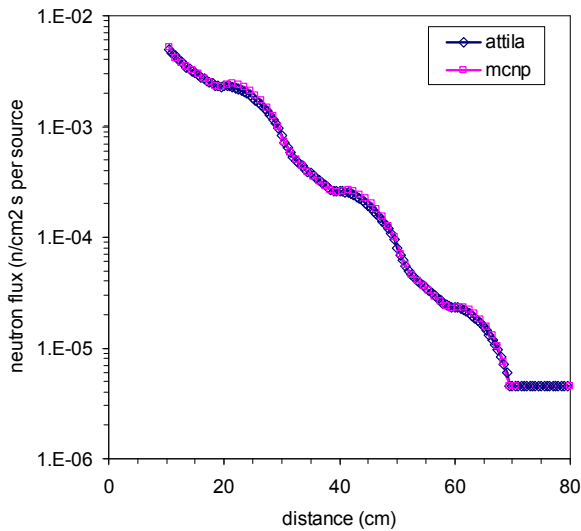


Fig. 9: total neutron flux results.

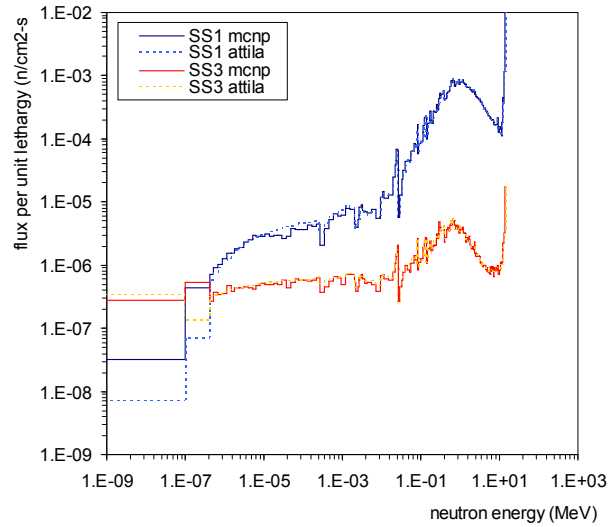


Fig. 10: neutron flux spectra at SS1 and SS3.

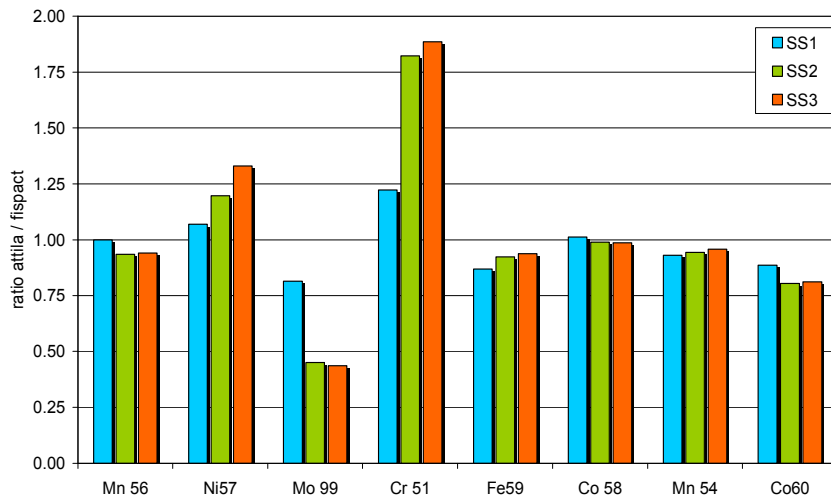


Fig. 11: ratio of ATTILA to FISPACT isotope production integrated over each steel slab for dominant nuclides at decay times of interest.

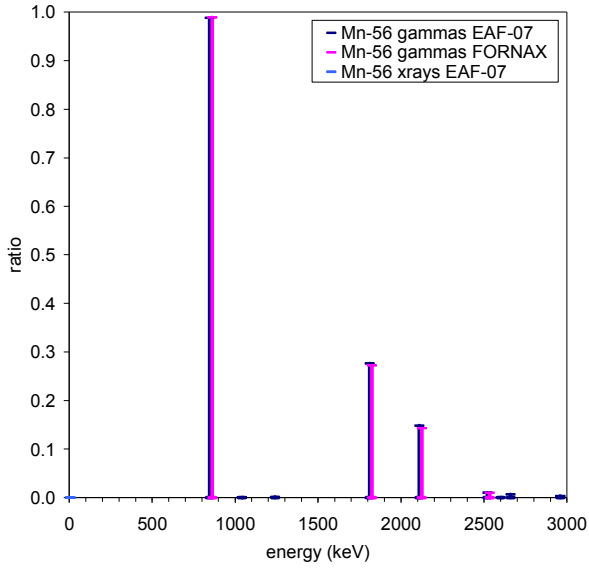


Fig. 12: decay gamma line info for Mn-56 in EAF-2007 and FORNAX XML data.

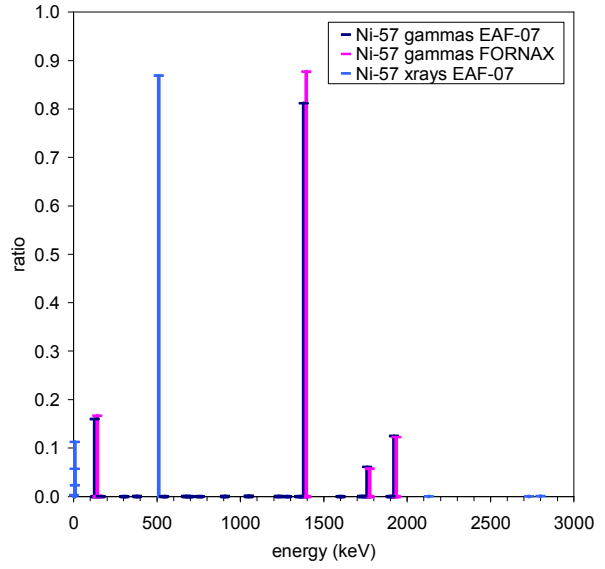


Fig. 13: decay gamma line info for Ni-57 in EAF-2007 and FORNAX XML data.

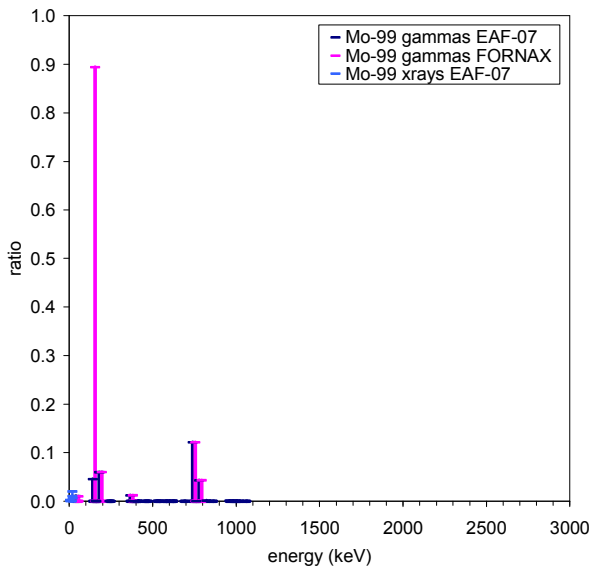


Fig. 14: decay gamma line info for Mo-99 in EAF-2007 and FORNAX XML data.

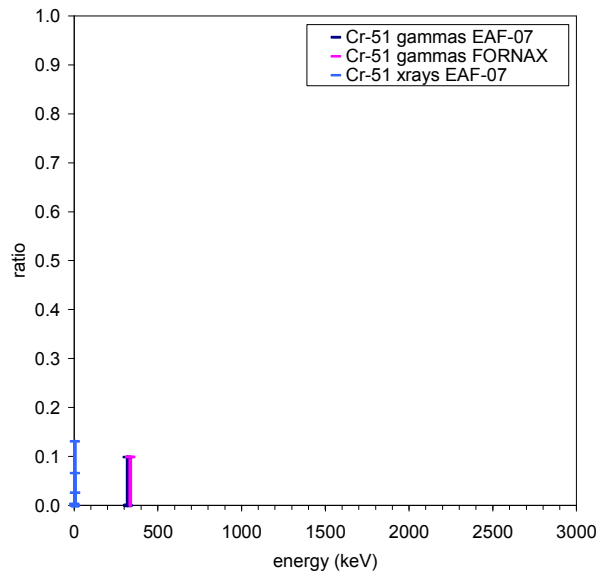


Fig. 15: decay gamma line info for Cr-51 in EAF-2007 and FORNAX XML data.

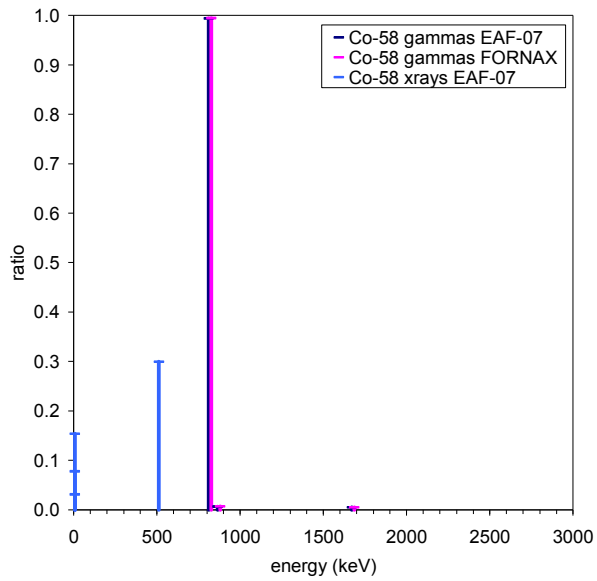


Fig. 16: decay gamma line info for Co-58 in EAF-2007 and FORNAX XML data.

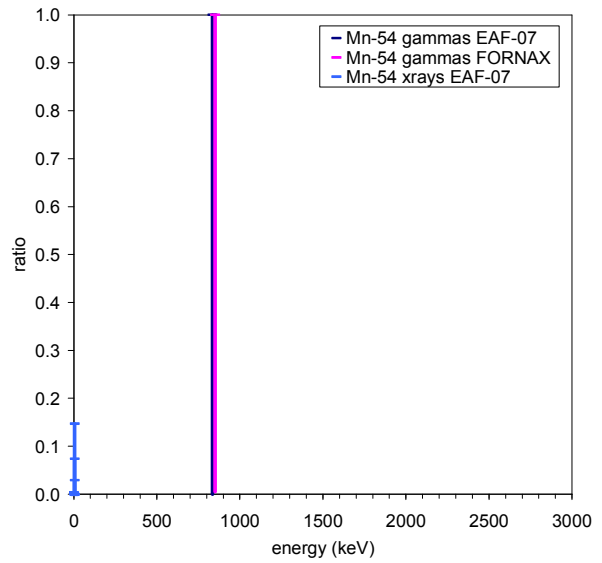


Fig. 17: decay gamma line info for Mn-54 in EAF-2007 and FORNAX XML data.

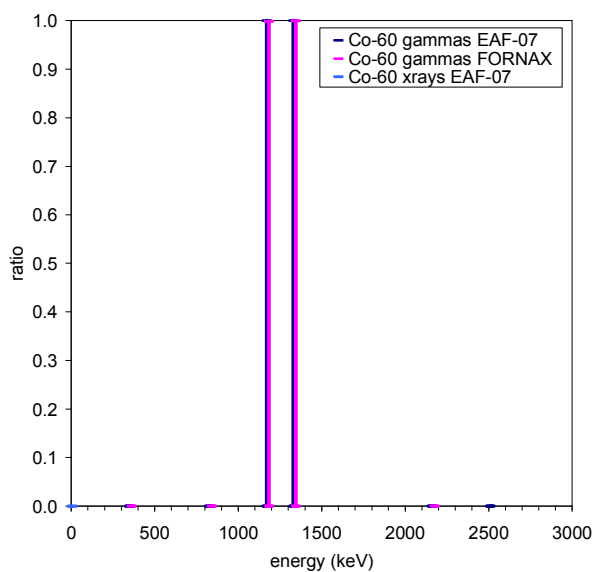


Fig. 18: decay gamma line info for Co-60 in EAF-2007 and FORNAX XML data.

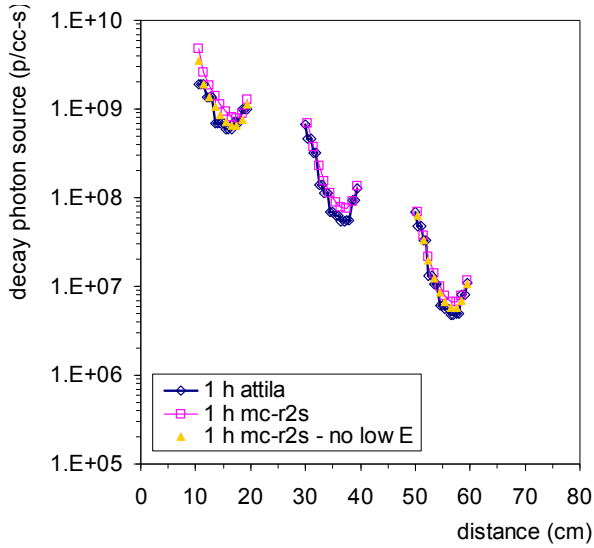


Fig. 19: ATTILA and MC-R2S decay photon source strength (p/cc.s) at 1 hour decay time.

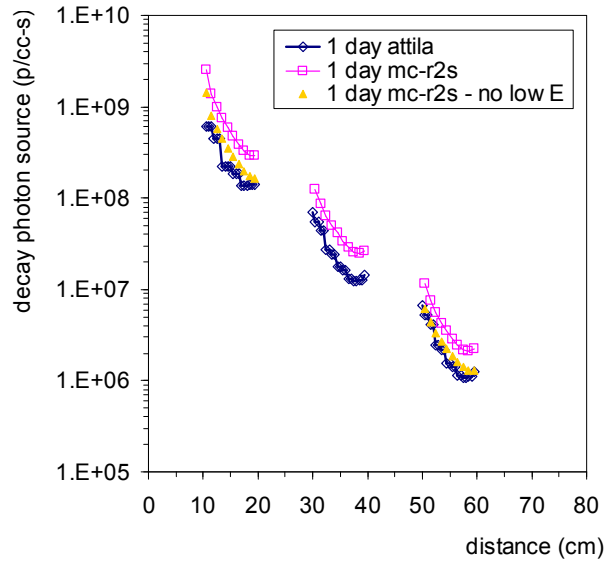


Fig. 20: ATTILA and MC-R2S decay photon source strength (p/cc.s) at 1 day decay time.

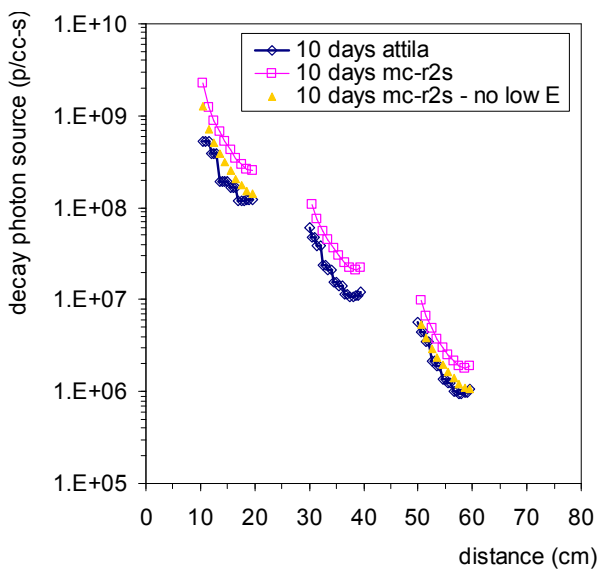


Fig. 21: ATTILA and MC-R2S decay photon source strength (p/cc.s) at 10 days decay time.

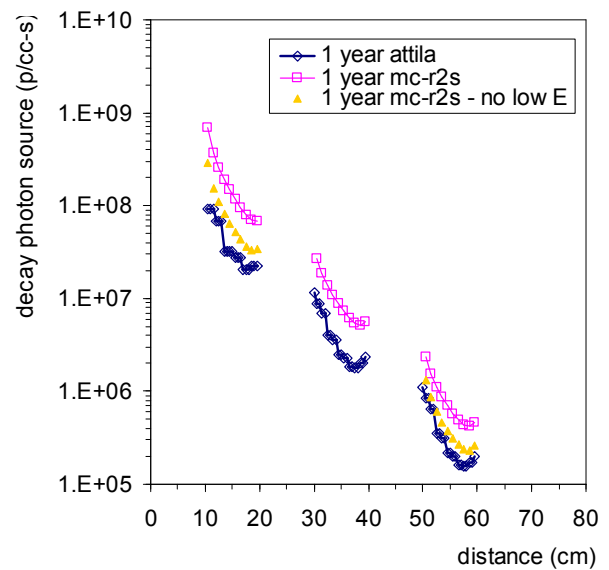


Fig. 22: ATTILA and MC-R2S decay photon source strength (p/cc.s) at 1 year decay time.

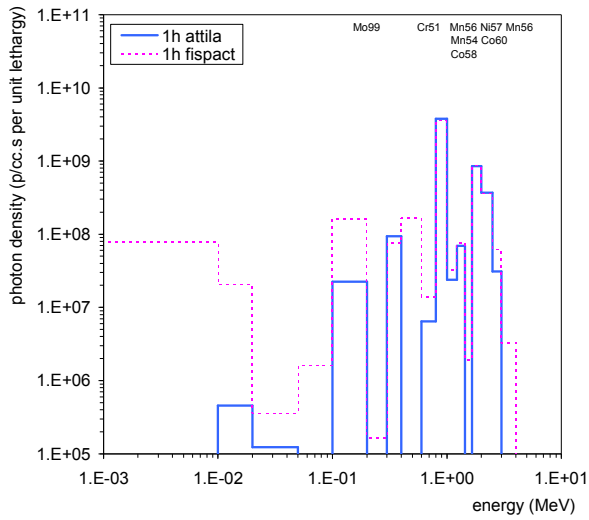


Fig. 23: ATTLA and FISPACT decay photon spectra integrated over SS1 at 1h decay time.

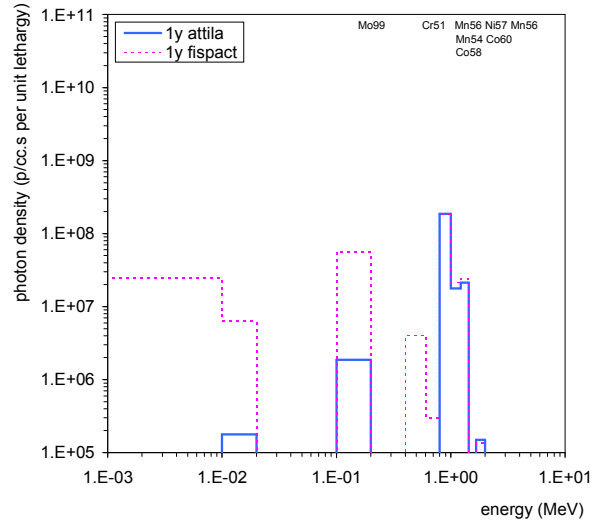


Fig. 24: ATTLA and FISPACT decay photon spectra integrated over SS1 at 1y decay time.

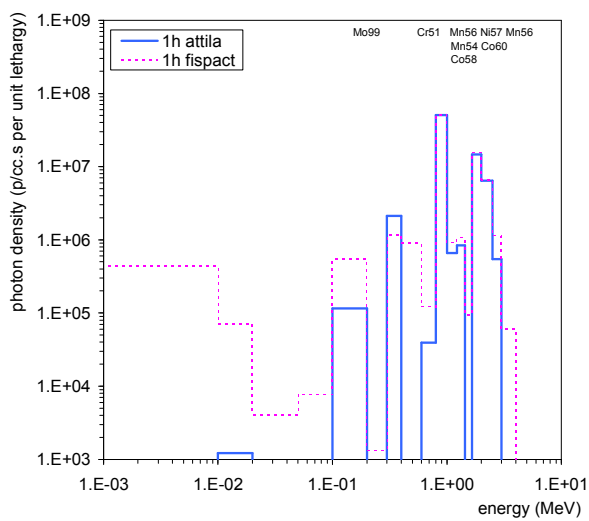


Fig. 25: ATTLA and FISPACT decay photon spectra integrated over SS3 at 1h decay time.

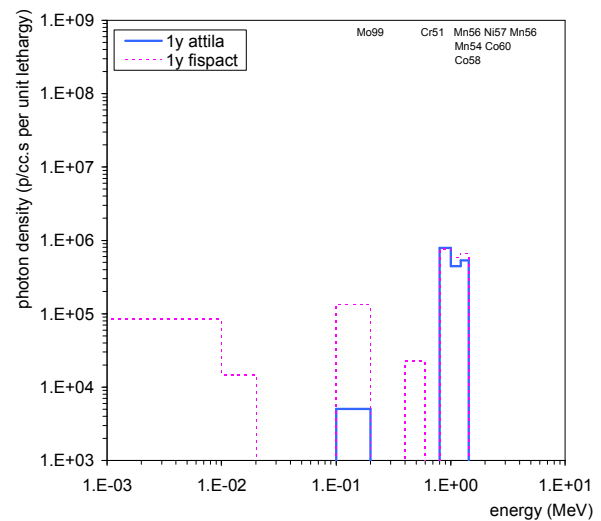


Fig. 26: ATTLA and FISPACT decay photon spectra integrated over SS3 at 1y decay time.

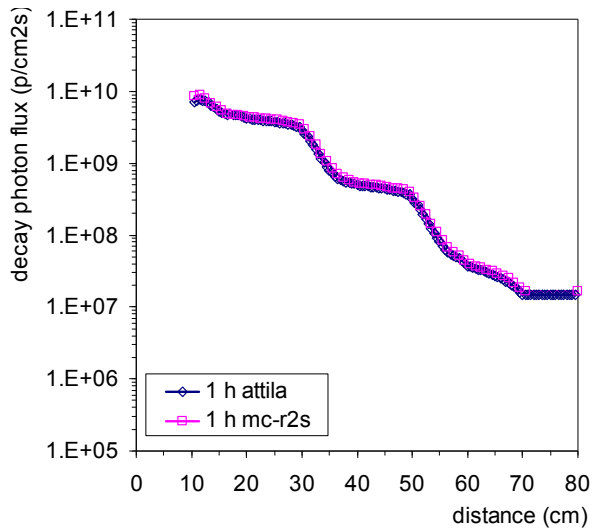


Fig. 27: ATTILA and MC-R2S total decay photon flux results at 1 hour (p/cm²s).

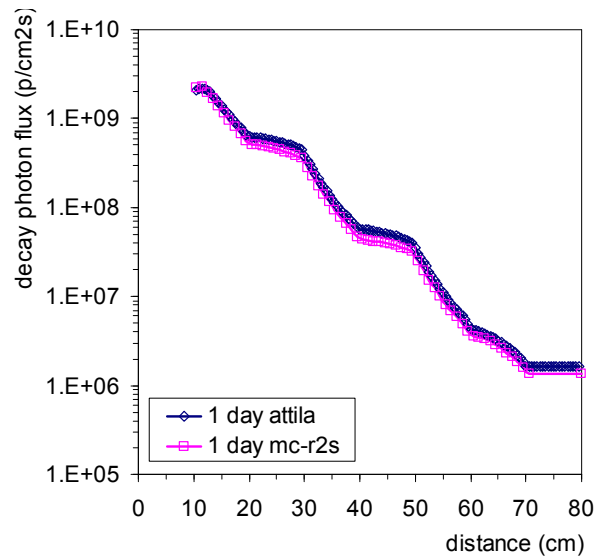


Fig. 28: ATTILA and MC-R2S total decay photon flux results at 1 day (p/cm²s).

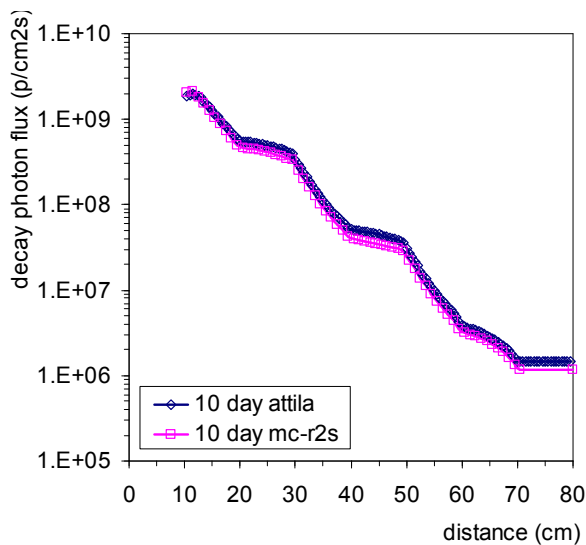


Fig. 29: ATTILA and MC-R2S total decay photon flux results at 10 days (p/cm²s).

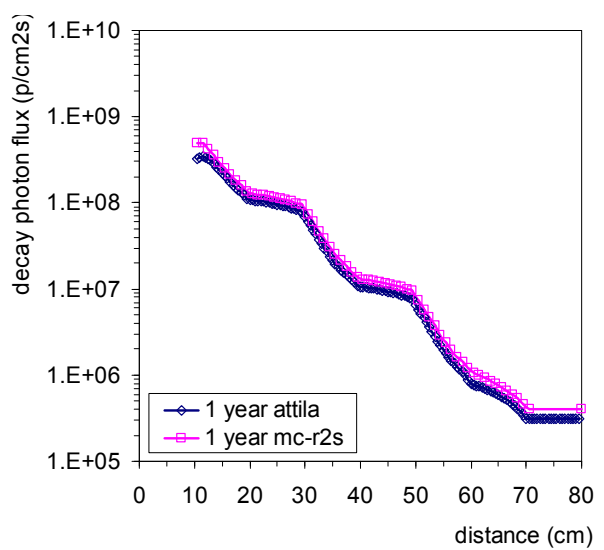


Fig. 30: ATTILA and MC-R2S total decay photon flux results at 1 year (p/cm²s).

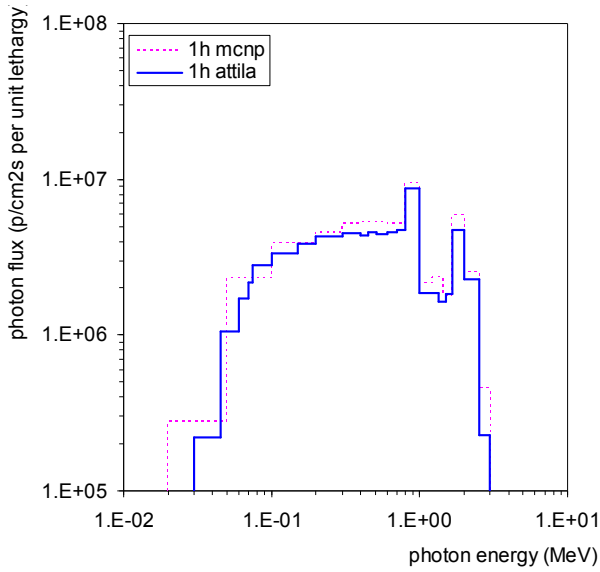


Fig. 31: MCNP and ATTILA decay photon spectra at rear air slab for 1 h decay time.

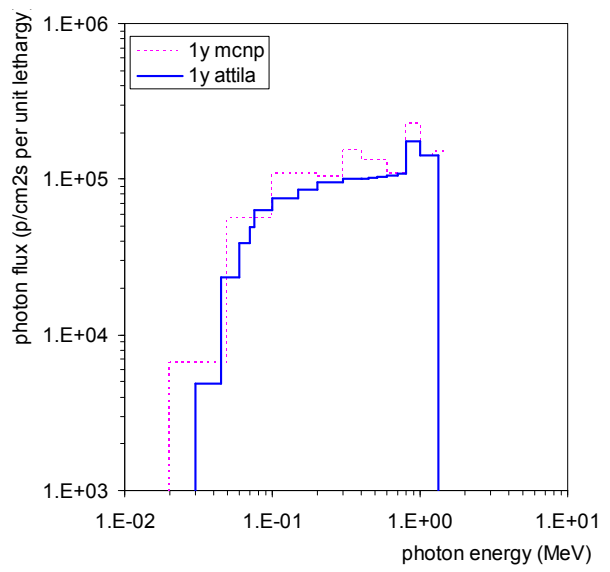


Fig. 32: MCNP and ATTILA decay photon spectra at rear air slab for 1 y decay time.

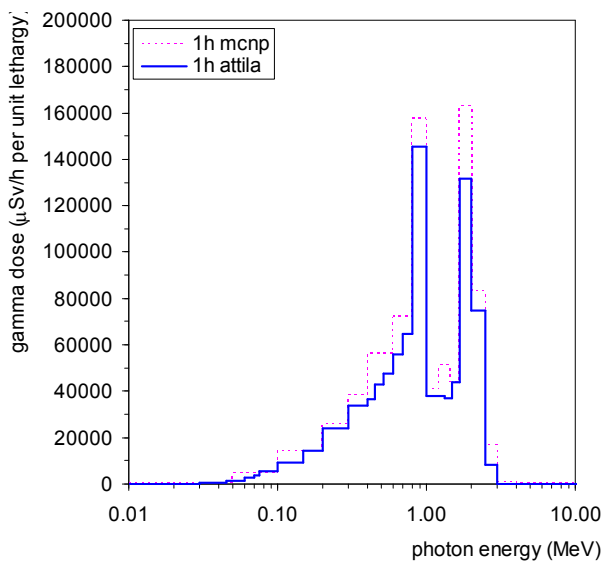


Fig. 33: MCNP and ATTILA decay gamma dose at rear air slab for 1h decay time, calculated using ANSI-ANS-1991 factors.

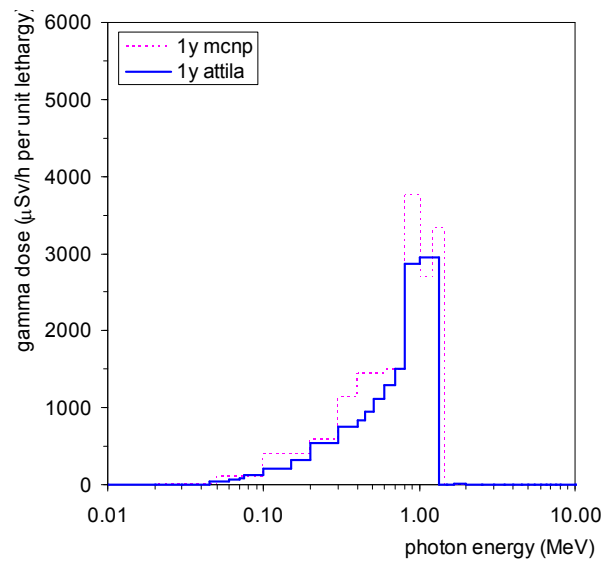


Fig. 34: MCNP and ATTILA decay gamma dose at rear air slab for 1y decay time, calculated using ANSI-ANS-1991 factors.

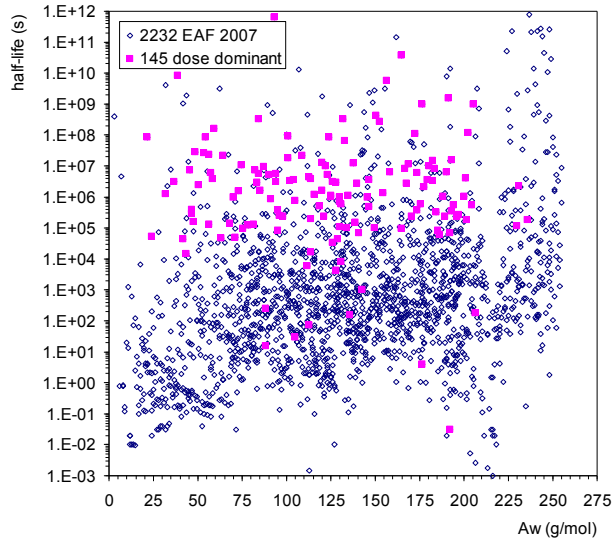


Fig. 35: EAF half-life (s) data for 2231 total nuclides and for 145 contact dose dominant nuclides.

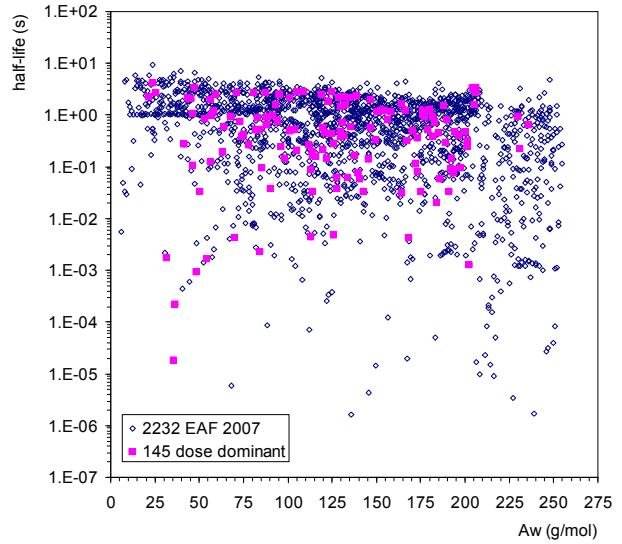


Fig. 36: EAF average gamma energy per decay (MeV) for 2231 total nuclides and for 145 contact dose dominant nuclides.

APPENDIX 1: MC-R2S FUNCTIONALITY

MC-R2S is a suite of UNIX script and FORTRAN routines coupling MCNP and FISPACT to perform the two transport and one activation calculations in the R2S method (see Figure A1). Thus MC-R2S relies on the powerful Monte Carlo method and the well-established MCNP code to perform the transport analyses, and on the thoroughly tested discrete ordinates method used by FISPACT and evaluated nuclear data of the EAF libraries for the activation step; details of these can be found in the user manuals, [A1,A2,A3].

The MC-R2S suite processes the output of a standard MCNP 5 neutron mesh tally to obtain neutron spectra at every voxel location, the only conditions on the mesh tally being that it must have rectangular geometry and be binned in energy to the VITAMIN-J standard. An additional MCNP run must be performed with the PTRAC output turned on, and from the PTRAC output file the distribution of different materials throughout the mesh is determined. Together with user-specified data such as the irradiation schedule, decay times and material compositions contained within the mesh volume, the script creates an appropriately mixed composition for each voxel location, which is passed to the inventory code FISPACT. Thus the activation section of the code automates the creation of FISPACT input files with appropriately weighted materials, decay times, and irradiation histories for each voxel. FISPACT is called to perform the activation runs. The FISPACT output of interest is the gamma-ray spectra at each decay time step; these spectra are also automatically extracted from the code’s output files and combined to define a spatially and energetically dependent decay gamma source for the subsequent, final MCNP photon run – including the correct source normalisation. The source definition is output in standard MCNP SDEF card format and hence is backwards compatible to MCNP 4C; no re-compilation of MCNP is required.

The system requirements of MC-R2S are a UNIX-like operating system, MCNP 5 (for the neutron run) and FISPACT 2007 (for activation). The FORTRAN programs are written in FORTRAN 77 and thus should compile with most compilers; specifically tested are the GNU “G77” and the INTEL “IFORT” compilers.

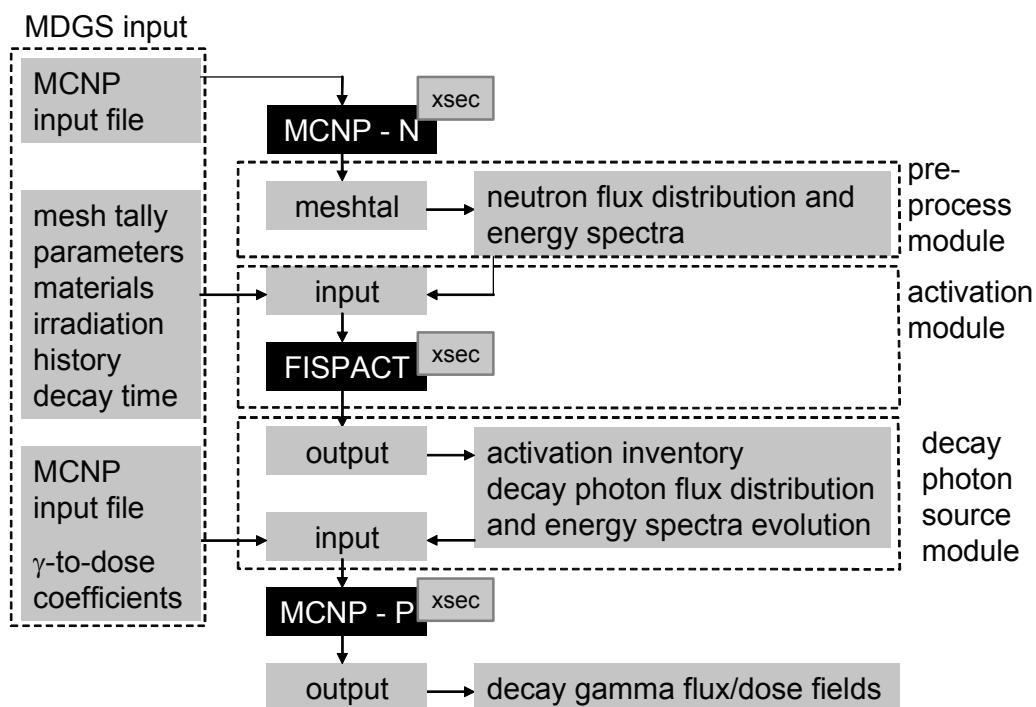


Fig. A1: MC-R2S flow chart.

The advantages of MC-R2S over preceding R2S software are, [A4]:

- Spatial resolution: the use of MCNP mesh-tallies allows for the necessarily fine spatial resolution required to capture intricacies of the neutron-induced activation field.
- Independency from geometry: the geometry representation in MCNP can be built without consideration of the activation and decay dose problems.
- Portability: the use of SDEF cards means the activation source can be used in most versions of MCNP without the need for recompilation of a source routine. Furthermore, it can be used in a different MCNP problem with varying boundary conditions, e.g. for investigation of the dose field in a room where the activated component has been placed after removal from the machine.

Currently, three limitations are observed:

- Firstly, the need for a rectangular mesh; at the moment, coupling of the problem and mesh geometries is only achieved exactly through rectangular approximation of the MCNP geometry representation, or approximately through great refinement of the mesh. This is reasonably practical in simple problems but will prove difficult to apply to large scale analyses.
- Secondly, the long run time employed in FISPACT runs is a severe limitation. At the moment, the minimum CPU time for a FISPACT run is ~15s in a conventional 2.00 GHz machine. For a typical mesh tally of ~100,000 elements (such as one covering a solid 1m³ geometry with a 3x3x3cm mesh) and one run per mesh voxel, the computational time required for the activation step in MC-R2S is of ~400h (!). Currently this issue is being tackled via implementing a pseudo-parallelisation of the FISPACT runs and the use of parallel computing. The possibility of coupling a faster but equally reliable activation code to the MC-R2S software, however, should not be disregarded.
- Finally, the length of the MCNP SDEF card can be a limiting factor for large meshes in 32-bit systems. At the moment this is being tackled by splitting the SDEF card and performing several photon runs. It is possible that an alternative route, i.e. the use of an auxiliary MCNP routine for the definition of the activation dose, be used in the future. This would entail that re-compilation of the code is in the end necessary, jeopardising its advantageous portability.

References

- [A1] X5 Monte Carlo Team, "MCNP – a general Monte Carlo N-Particle transport code: version5 user's guide", LANL report LA-CP-03-0245, October 2005.
- [A2] R.A. Forrest et al., "FISPACT 2007 user manual", UKAEA **FUS 534**, March 2007.
- [A3] R.A. Forrest et al., "EAF 2007 neutron-induced cross section library", UKAEA **FUS 535**, March 2007.
- [A4] Y. Chen et al., "Rigorous MCNP based shutdown dose rate calculations: computational scheme, verification calculations and applications to ITER", *Fus. Eng. and Des.*, **63–64** (2002), p107.

APPENDIX 2: ATTILA ASG FUNCTIONALITY

2.1 FORNAX activation solver method

The FORNAX module, which performs the nuclear transmutation calculations, is designed to interface directly with ATTILA. The purpose of FORNAX (Latin for "furnace") is to solve the Bateman equations for the build-up, consumption, and decay of nuclides in a neutron radiation field. The Bateman equations are a coupled set of first order ordinary differential equations of the form:

$$(d/dt)N(t) = \text{formation rate from decay of a parent nuclide} + \\ \text{formation rate from transmutation of precursor nuclides} - \\ \text{loss rate from transmutation} - \\ \text{loss rate from radioactive decay}$$

$N(t)$ is a vector of nuclide concentrations (i.e. atom-densities) and d/dt is the derivative with respect to time. The loss rates from transmutation and radioactive decay are proportional to the concentration of the particular nuclide. The formation rates from parent decay and precursor transmutation are proportional to the concentration of particular precursor nuclides. This results in coupling of the differential equations. The transmutation rates are proportional to the neutron flux which results in a coupling of the equations to the transport solution. In general, N is a function of space due to differences in precursor concentrations and the variation of the neutron flux magnitude and spectrum throughout the problem. Also N has a time dependence on the neutron flux. In FORNAX, the initial precursor concentrations are assumed to be constant throughout the computational volume and the neutron flux is assumed to be constant throughout the volume and the time-step. These assumptions allow the transmutation terms to be written as constants and essentially removes the spatial dependence of the concentrations within the computational volume. Thus, the entire system of equations can be written as:

$$(d/dt)N(t) = A.N(t)$$

where A is a matrix of constant coefficients. This system of equations has a simple, analytic solution:

$$N(t) = N_0 \exp(A.t)$$

The mathematical definition of the exponential of a matrix is somewhat arcane, but it has a straightforward representation. If A is diagonalizable, then it can be expressed as:

$$A = PDP^{-1}$$

where D is a diagonal matrix. The exponential term then becomes:

$$\exp(A.t) = P.\exp(D.t).P^{-1}$$

where $\exp(D)$ is just the exponential of the coefficients on the diagonal of D . Expressing a matrix in diagonal form entails finding its eigenvalues. For the general case of FORNAX, A is approximately 1312 x 1312. The eigenvalues of A are therefore found as the roots of a 1312-degree polynomial.

There are several ways to attack this problem, but most of them involve iteration on the matrix to extract the eigenvalues, which can be computationally intensive. As an alternative

to the calculation of the coefficient matrix eigenvalues, FORNAX uses a Taylor series expansion to represent the matrix exponential:

$$\exp(A.t) = I + (A.t) + \frac{1}{2} (A.t)^2 + \frac{1}{6} (A.t)^3 + \dots$$

These straight-forward matrix equations are rewritten in terms of recursion relations for each nuclide so that it is not necessary to store any copies of the entire 1312 x 1312 matrix. The code retains only the number of terms in the series required to meet a 0.1% accuracy requirement. In order to reduce the stiffness of the system, nuclides with very short half-lives are removed and solved separately. This separation gives rise to advice to break down a burn-up step into several sub-steps so that the short-lived nuclides can "catch up".

This technique is similar to that used in the ORIGEN [A1] burn-up solver available from Oak Ridge National Laboratory. There are many modern packaged systems, both commercial and free, for solving large systems of ODEs; for example the "SUNDIALS ODE Solver" (<http://www.llnl.gov/CASC/sundials/>), or the "ODEPACK ODE Solver" (<http://www.llnl.gov/CASC/odepack/>) from Lawrence Livermore National Laboratory. These solvers include both direct and numerical versions. Other advanced solution techniques may be applicable as well; for example the Krylov based solution technique, [A2].

FORNAX solves the Bateman system described above for a single region (depletion-zone) and time-step. In ATTILA, a depletion zone consists of a single tetrahedral cell. Input is provided in the form of flux, cross section, and atom density link files specifying:

- initial isotope concentrations (N_0) on each depletion zone,
- multi-group scalar flux (ϕ_g) on each depletion zone,
- time-step size (Δt), and,
- optionally: a file containing energy group bounds and any reaction cross sections provided by ATTILA to replace the default values in the XML data library.

FORNAX computes the concentration for all of the listed nuclides in the light element, actinide, and fission product libraries. FORNAX writes new concentrations, $N(t)$ to an atom density link file for access by ATTILA for cross section computation during the course of the transport calculation. ATTILA can normalize the results of the transport calculation to the user specified power level and write a scalar flux link file for use by FORNAX on the subsequent time step. ATTILA will also compute a flux shape at the end of each time cycle, and at the beginning of any time cycle for which a geometric configuration change has been specified. Finally, a gamma-ray source specification is also produced that represents radiation emitted by decaying nuclides.

Information regarding the decay and daughter chains that can be produced in a particular problem is assumed to be available at the time the cross section file is created. For accurate results, the DTF data file should include all the isotopes in the clean problem, and all the burn products deemed to be neutronically significant that can arise from the original clean isotope list. Note that cross section data on the default FORNAX data file is used strictly for FORNAX internal reaction rate computations and does not directly enter into the transport calculation. Any isotopes that the user desires to be used in the burn or transmutation calculation in place of the default cross sections provided in the internal burn module data files should be listed on the DTF file. This default cross section data will automatically be replaced by DTF cross section data for any isotope that appears on the DTF file. ATTILA reaction cross sections in burn regions are initially set as specified by the user. Subsequently, burn region cross sections are computed by looping over all isotopes listed in the DTF file and folding these into the FORNAX supplied isotopic atom densities.

2.2 ATTILA ASG guidance for a calculation

The activation process recently implemented in ATTILA is essentially an R2S calculation performed in consecutive steps, [A3]:

- Step 1: neutron transport calculation – solves for the detailed neutron flux field.
- Step 2: activation source calculation – generates one or more activation source files.
- Step 3: activation dose field calculation – solves for the dose field resulting from the activation source.

Steps 1 and 3 can be performed entirely through the ATTILA graphical user interface (GUI). Step 2 is invoked through modifications to the input file used in Step 1 and created by the ATTILA GUI. A description of the process and of the FORNAX activation solver follows.

Step 1: neutron transport

Step 1 is a conventional neutron transport calculation. There are no special requirements for this calculation, other than:

- The calculation has to be performed solving all groups in the cross section file. That is, all groups in the cross section set should be run, without group collapse. The “fendl_29n” cross section set is a 29 group neutron set created from FENDL 2.1 data, collapsed using a representative fusion spectrum; this is the recommended set for the step 1 calculation when memory requirements are a concern.
- The terminal restart file should be output, as the activation program will read the neutron field data from the terminal restart file as input to step 2.

At the time of this calculation, no activation specific parameters need to be applied, and this calculation can be set up entirely through the GUI. Thus, this calculation may be performed to obtain any number of results, with various solution edits, which are independent of a subsequent activation calculation.

Step 2: activation source calculation

At present, the activation capability is not supported through the GUI. Calculation parameters for the activation are specified directly in the ATTILA input deck. The following steps should be performed, following a “run1” calculation from step 1 (names are indicative only):

- create a new directory at the same level as the run1 directory from step 1, called “run2-activation”.
- copy the “attila.inp” file from the run1 directory into run2-activation;
- open the newly copied attila.inp file in the run2-activation directory with a text editor, and make the changes described below:
 - In the input_file_block:
 - remove the line specifying the volume source file, as this is not needed for the activation:
 - ✓ delete the line: [volume_source_file “run1.vsrc.inp”]
 - specify the starting flux file from run1, by adding the following line:
 - ✓ add the line: [starting_flux_file “./run1/run1.flux_mom.trm”]
 - In the output_controls_block:

- turn off the output of the terminal restart file:
 - ✓ add/change the line: [write_terminal_rs_file .false.]
 - turn on the output of the activation source file:
 - ✓ add the line: [write_activation_source_file .true.]
 - In the transport_controls_block:
 - read the solution file from the terminal restart file:
 - ✓ add/change the line: [starting_moments disk_file]
 - In the iterations_controls_block:
 - accept the initial solution field (from step1), so no transport iterations are performed:
 - ✓ add/change the line: [accept_initial_solution .true.]
 - specify the activation parameters, through the command nuclear_transmutation_time_steps; this command specifies the activation parameters: (1) number of time steps, (2) duration of each time step, and (3) whether each time step corresponds to a 'burn' or 'decay' mode. The syntax is as follows:
 - ✓ line 1: nuclear_transmutation_time_steps n_steps
 - § n_steps – the number of time steps to be performed
 - ✓ lines 2 through n_steps+1: dt scale_factor keep
 - § dt – real argument giving the time step duration (days)
 - § scale_factor – real argument describing the burn or decay; a value of 0.0 specifies the time step as 'decay'; for a 'burn' time step, a value of 1.0 should be prescribed if the calculation performed in step 1 used the non-normalized source intensity; if the source intensity in step 1 was normalized, a scale factor should be prescribed which will scale the original source intensity up to the actual value.
 - In the mesh_region_definition_block:
 - specify the mesh regions in which the activation is performed, through the burn_region_def command. The syntax is identical to that of the region_def command. For activation calculations, the user will simply replace the region_def command with burn_region_def for every region in which the activation is to be performed, without changing any of the associated arguments. If activation is to be performed for all the mesh regions in a model, a global find and replace can be performed to replace "region_def" with "burn_region_def". No changes should be made to the arguments of this command.
 - Once the above changes are complete, save the changes to attila.inp and exit the editor. The ATTILA solver is then run from the command line in the run2-activation directory. For Linux, this is performed from the command prompt by typing "attilaSolver".

The primary output of the activation routines is a separate ATTILA volume source file ("run2-activation.vsrc.inp") written for each activation time step: i.e. an activation source for each time step. Each source file contains the gamma activation source at the completion of the corresponding time step. These volume source files are stored in separate subdirectories

created during the activation calculation, which are named `fornax_cycle_#`, where # refers to the corresponding time step.

Step 3: activation dose field calculation

In step 3, an ATTILA calculation is performed to calculate the dose field resulting from the desired activation source generated in step 2. In general, the activation source from the last activation time step is used as input, though the source from any time step could in principle be used. This calculation can be set up entirely through the ATTILA graphical user interface. Some major features of this calculation are as follows:

- This is generally a gamma only calculation, and neutron groups may be collapsed out for the calculation.
- This calculation must use the same computational mesh as that used for step 1. The activation source file is specific to the computational mesh.
- There is no requirement that material properties are the same as those used in step 1. For example, step 1 may be performed to compute the activation source in a single component out of a large assembly. In step 3, materials in all of the other components could be changed to air, which would be equivalent to simulating the dose field from that single component if it was removed from the assembly and placed in an empty room (e.g. a hot cell).
- There is no requirement for the same cross section set to be used as that in step 1. If a neutron-only cross section set was used for step 1, such as the `fendl_29n` set, this must be replaced by a set which contains gammas.

Note that when the cross section set in a calculation is changed, the material composition data (specified in the Material Editor tab) will automatically be removed. Provisions must be made beforehand if this information is not to be lost (e.g. renaming cross section files). The major steps for performing this calculation are discussed below:

- Launch the Attila graphical user interface and open the project used for in step 1.
- Duplicate the calculation used in step 1:
 - Right click on the run1 calculation icon Duplicate
- Next, edit the duplicated calculation, which should be named run2:
 - Right click on the run2 calculation icon Edit
- Once in the calculation editor, make the following changes:
 - In the General tab, rename the calculation to run3
 - In the Cross Section Library tab, select an appropriate cross section set which contains gamma cross sections in the desired energy ranges.
 - In the Cross Sections Options tab, select User Specified under Energy Group Limits, then select the desired gamma groups to be included in the calculation.
 - In the Volume Source tab, select the From File button, then select the `run1.vsrc.inp` file from the appropriate activation step subdirectory.
 - User defined custom reports, for quantities such as dose, may be specified as desired. A custom report can optionally be created to output the resulting activation source, which can be performed to verify that the activation was performed correctly.

- Once the above changes are complete, save the changes and launch the calculation from the graphical user interface.

References

- [A1] O.W. Hermann et al., "ORIGEN-S: SCALE system module to calculate fuel depletion, actinide transmutation, fission product buildup and decay, and associated radiation source terms", ORNL report, ORNL/NUREG/CSD- 2/V2/R6, March 2000.
- [A2] M. Hochbruck et al., "On Krylov subspace approximations to the matrix exponential operator", *SIAM J. on Num. Anal.* **34-5** (1997) p1911.
- [A3] J.M. McGhee, T.A. Wareing, D.A. Barnett Jr. and K.G. Thompson, "ATTILA V6 user manual", Transpire Inc. – in preparation.

APPENDIX 3: FISPACT CONTACT DOSE APPROXIMATION

Accounting for the necessarily fine spatial resolution, the R2S method provides a reliable to map the shutdown dose field throughout an entire geometry. Due to the decay gamma source being intricately distributed and dependent on the effect of a varying neutron field on different materials, any approximation is bound to have little realistic application. For rough evaluations, however, FISPACT has a built-in capability to estimate the gamma dose arising from the radioactive decay of the nuclides in an irradiated material, which has been widely used whilst no better tools were available. The estimation is made via the so-called “contact dose” approximation, which consists in calculating the dose in air at the surface of a semi-infinite slab having constant specific activity and radionuclide composition equal to that of the material that is to be analysed. This approximation, essentially a zero-dimensional formulation, has an exact analytical solution in terms of the specific activity, [A1]:

$$D = 5.76 \cdot 10^{-10} \frac{B}{2} \sum_{i=1}^{24} \frac{\mu_a(E_i)}{\mu_m(E_i)} S_v(E_i)$$

$$S_v = E_g N_g A(t)$$

where D is surface dose in Sv/h, E_i mean energy of group i , μ mass attenuation coefficient of air (a) or material (m), B build-up factor, S_v rate of gamma emission in MeV/kg.s, E_g gamma energy in MeV, N_g line intensity and A specific activity. The build-up factor is a mathematical artefact accounting for scattered radiation in shielding applications, and has a default FISPACT value of 2.

The contact dose approximation provides valuable information for the comparison of the shutdown dose between different materials and neutron flux, and combined with powerful software such as FISPACT it can be used to investigate dominant nuclides and reaction pathways responsible for the activation dose, as shown in other parts of this document. The conditions assumed, however, are afar from those encountered in a real activation problem with a largely distributed and spatially variable decay gamma source. Firstly, the contact dose approximation does not take into account the real 3D geometry of the problem. Furthermore, the contact dose approximation does not account for variable activation levels within the geometry of interest; in most real situations of neutron-induced activation, neutrons are attenuated at an approximately exponential rate as they travel from the source and into the material, and the activation levels decay accordingly. This effect is generally small due to the small mean free path of gamma rays in most materials, however it is still reasonable to expect that the contact dose approximation will overestimate the dose in regions of the geometry where the activity is decaying with depth (e.g. plasma facing components) and underestimate it in regions where the activity increases with depth (e.g. at the rear of a thick shield) as a result of its over or under-estimation of the activity level, respectively; this is illustrated in Figure A1.

Table A1:

dose (mSv/h)	SS1 front MC-R2S R2S method	SS1 front FISPACT contact dose	SS3 rear MC-R2S R2S method	SS3 rear FISPACT contact dose
1 hour	67,000	126,000	555	460
1 day	14,400	29,000	39.4	30
10 days	13,600	27,000	34.8	27
1 year	2,800	5,000	12.7	8.7

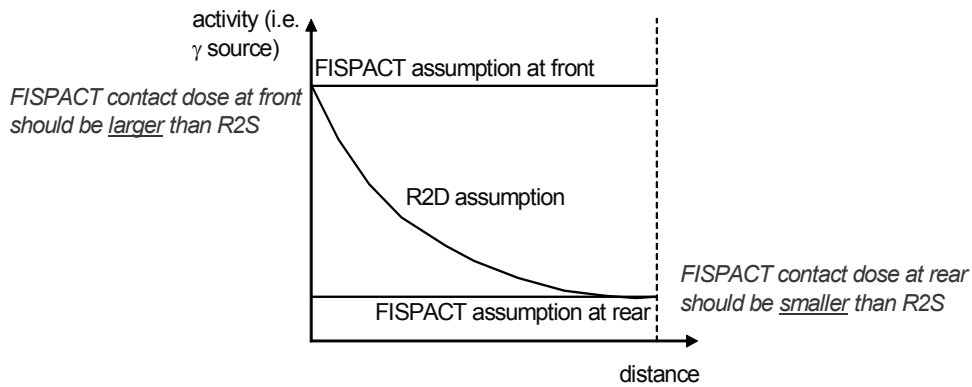


Figure A1.

This feature can be exemplified using the results of the problem analysed in this document, which provide unbiased comparison given its 1D nature; i.e. 3D effects are suppressed. Comparison of the contact dose results of the FISPACT output with the values obtained through the meticulous R2S method is made in Table A1. Note that the “rear” results do not correspond to the air slab, as in previous parts of the document, but to the rear of the SS3 steel slab; this is so that proper comparison can be made with steel activation results from FISPACT: water activation is negligible in comparison.

As expected, the contact dose approximation in FISPACT over-estimates the dose at the front of the model, i.e. the source-facing side from which activation levels decay; conversely, it under-estimates the dose at the rear. It is interesting to notice that the over-prediction is much larger than the under-prediction; this result is related to the fact that whereas the actual gamma source profile of the test problem at the front does fit the assumption in Figure A1, this is not so much the case at the rear according to Figures 19 – 22 in the document. Another issue is the constant build-up factor used in the above formulae. In other applications and dosimetric software, variable build-up factors are used depending on the geometry and gamma energy, [A2].

References

- [A1] R.A. Forrest, “FISPACT 2007 user manual”, UKAEA **FUS 534**, March 2007.
 [A2] G.F. Knoll, “Radiation detection and measurement”, Wiley&Sons, 2004.